European Journal of Medicinal Chemistry 223 (2021) 113677

Contents lists available at ScienceDirect

European Journal of Medicinal Chemistry

journal homepage: http://www.elsevier.com/locate/ejmech

Discovery of a potent MLL1 and WDR5 protein-protein interaction inhibitor with *in vivo* antitumor activity

Weilin Chen [a, b], Xin Chen [a], Dongdong Li [a], Xianghan Wang [a], Guanlu Long [a], Zhengyu Jiang [a, c, ***], Qidong You [a, c, **], Xiaoke Guo [a, c, *]

[a] Jiangsu Key Laboratory of Drug Design and Optimization and State Key Laboratory of Natural Medicines, China Pharmaceutical University, Nanjing, 210009, China
[b] Department of Medicinal Chemistry, School of Pharmacy, Nanjing Medical University, Nanjing, 211166, China
[c] Department of Medicinal Chemistry, School of Pharmacy, China Pharmaceutical University, Nanjing, 210009, China

ARTICLE INFO

Article history:
Received 6 May 2021
Received in revised form
18 June 2021
Accepted 25 June 2021
Available online 28 June 2021

Keywords:
MLL1-WDR5 interaction
Phenyltriazole scaffold inhibitor
Antitumor
MLL1 HMT activity

ABSTRACT

MLL1-WDR5 interaction is essential for the formation of MLL core complex and its H3K4 methyltransferase activity. Disrupting MLL1-WDR5 interaction has been proposed as a potential therapeutic approach in the treatment of leukemia. A "toolkit" of well-characterized chemical probe will allow exploring animal studies. Based on a specific MLL1-WDR5 PPI inhibitor (**DDO-2117**), which was previously reported by our group, we conducted a bioisosterism approach by click chemistry to discover novel phenyltriazole scaffold MLL1-WDR5 interaction blockers. Here, our efforts resulted in the best inhibitor **24** (**DDO-2093**) with high binding affinity (K_d = 11.6 nM) and with improved drug-like properties. Both *in vitro* and *in vivo* assays revealed **24** could efficiently block the MLL1-WDR5 interaction. Furthermore, **24** significantly suppressed tumor growth in the MV4-11 xenograft mouse model and showed a favorable safety profile. We propose **24** as a chemical probe that is suitable for *in vivo* pharmacodynamic and biological studies of MLL1-WDR5 interaction.

1. Introduction

Mixed-lineage leukemia 1 (MLL1) belongs to the SET1 family of methyltransferases, and it catalyzes the mono-, di-, and trimethylation of histone 3 lysine 4 (H3K4) as well as facilitates transcriptional initiation [1–4]. MLL1 is frequently misregulated in various forms of human acute leukemia, with a common gene translocation at chromosome 11q23, leading to the fusion of the *MLL1* gene with other genes, and this is associated with cancers and developmental disorders [5,6]. Chromosome arrangements result in leukemogenic MLL1 fusion proteins. MLL1 fusion proteins lack the C-terminal SET domain and thus cooperate with wild-type MLL1 to catalyze H3K4 HMT enzymatic activity as well as active *HOXA9* and *Meis1* gene expression, thus leading to leukemogenesis [7–11]. Therefore, targeting the H3K4 HMT activity of MLL1 has emerged as a tractable approach to treat leukemia carrying MLL1 fusion protein.

The HMT enzymatic activity is very weak when the MLL protein is present in isolation. However, formation of the MLL1 core complex, containing WDR5 (WD repeat domain 5 protein), RbBP5 (Retinoblastoma Binding Protein 5), and ASH2L (Absent, Small, or Homeotic-2-Like), dramatically enhances the enzymatic activity [12–16]. WDR5 is particularly crucial to maintain the integrity and catalytic activity of MLL1 complex [17–19]. Hence, using inhibitors to disrupt the protein-protein interaction (PPI) between MLL1 and WDR5 may be a potential approach to treat MLL1-dependent leukemia, which is associated with a high tumor grade, poor survival, and insensitivity to chemotherapy.

Up to now, two major classes of inhibitors disturbing MLL1-WDR5 interaction have been reported. The first class was peptidomimetics which was commenced by the report of minimum peptide **1** (**Ac-ARA-NH_2**) [20]. Further modification of **Ac-ARA-NH_2**

* Corresponding author. Jiangsu Key Laboratory of Drug Design and Optimization and State Key Laboratory of Natural Medicines, China Pharmaceutical University, Nanjing, 210009, China.
** Corresponding author. Jiangsu Key Laboratory of Drug Design and Optimization and State Key Laboratory of Natural Medicines, China Pharmaceutical University, Nanjing, 210009, China.
*** Corresponding author. Jiangsu Key Laboratory of Drug Design and Optimization and State Key Laboratory of Natural Medicines, China Pharmaceutical University, Nanjing, 210009, China.
E-mail addresses: jiangzhengyucpu@163.com (Z. Jiang), youqd@163.com (Q. You), kexin95@126.com (X. Guo).

https://doi.org/10.1016/j.ejmech.2021.113677
0223-5234/

peptide yielded several linear and cyclic peptidomimetics with high affinity to WDR5, including peptide **2 (MM102)** and peptide **3 (MM589)** (Fig. 1A) [21–23]. In addition, several nonpeptides, such as small molecule inhibitor **4 (WDR5-0101)**, were disclosed to block MLL1-WDR5 PPI by high throughput screening Ontario Institute for Cancer Research general screening library [24]. Then more potent compounds were obtained based on the cocrystal structures of the inhibitors with WDR5 protein [25–30]. Compound **5 (OICR-9429)** showed high binding affinity to WDR5 and was explored for the treatment of CEBPA mutant AML [26,27]. Meanwhile, the biphenyl scaffold inhibitor **6 (DDO-2117)** with high affinity to WDR5 protein (IC_{50} = 7.6 nM) was reported by our group (Fig. 1B) [28]. Different from the above blockers, **7 (6e)** was a new small molecule targeting the Win site of WDR5 [31]. In 2020, another nonpeptide **8** (compound **16**) was reported to exert antitumor activity against MYC-driven cancer cells through inhibition of WDR5-MLL1 PPI with a K_d value of 0.02 nM [32,33]. Although these inhibitors showed very high affinity with WDR5 *in vitro*, there was no *in vivo* studies reported up to now. Therefore, our further work is to discover novel compounds with suitable physicochemical properties and explore their bioactivities *in vivo*. Here, we designed a series of compounds containing a phenylalkynyl scaffold aimed at reducing the rigidity of biphenyl molecules and improving the aqueous solubility by a bioisosterism approach from biphenyl compound **6** [28]. Considering that the phenyltriazole compounds could be prepared from alkyne and azide by click chemistry, we also designed and synthesized some phenyltriazole compounds. The phenyltriazole compounds retained high binding affinity to WDR5 *in vitro*, moderate antiproliferation activity against human acute leukemias cells harboring MLL fusion protein and low toxicity against noncancerous human cells. The most potent compound **24** selectively inhibited MLL1 HMT activity *in vitro*. Meanwhile, **24** effectively downregulated H3K4 methylation level and reduced the expression levels of MLL-fusion protein dependent genes in cells. In addition, **24** not only displayed good drug-like properties but also exhibited significant *in vivo* activity in the MV4-11 xenograft model. Notably, it had a large therapeutic window with no significant subacute toxicity in mice treated with four times of the efficacy dose. These results suggested that MLL1-WDR5 PPI inhibitors can achieve potential anticancer therapeutic effects with preferable safety. **24** (**DDO-2093**) appeared to be a useful chemical probe of MLL1-WDR5 PPI suitable for being studied *in vivo*.

2. Results and discussion

2.1. Structure-based bioisosterism yields phenylalkynyl compounds

Despite the high binding affinity of compound **6** to WDR5 protein *in vitro* [28], **6** was not suitable for further studies due to its poor permeability (1.6×10^{-6} cm/s, pH = 7.4). Simultaneously, most of the biphenyl compounds showed poor aqueous solubility. Further improvements in pharmaceutical properties need to be made in order to demonstrate the *in vivo* therapeutical potential of MLL1-WDR5 PPI inhibitors. We hypothesized that the biphenyl scaffold may contribute to the poor solubility due to its structural bulkiness and rigidity. In an attempt to reduce the molecular rigidity and discover a new fragment to replace the biphenyl moiety, we embarked on a bioisosterism approach utilizing the structural information of inhibitors binding to WDR5 protein. The detailed analysis of the binding site for the biphenyl scaffold with WDR5 protein has been reported by our group [28]. The 5-amino-2-chloro-4-fluoro-3-methyl-*N*-(2-(4-methylpiperazin-1-yl)phenyl) benzamide moiety of compound **6**, binding to the deepest part of the Win site of WDR5 protein, was incorporated into the new compound design for consistency in activity comparisons. The hydrophobic interaction between Phe133, Phe149, Tyr191 and aromatic ring A (Fig. 2) promoted the binding strength and a linear structure at this position was also necessary. Therefore, we decided to incorporate a conformation restriction to maintain the linear structure and retain the hydrophobic interaction using a propargyl moiety. Conversely, the 4-position moiety was positioned toward the solvent accessible area, where further modifications were feasible for incorporation of physicochemical property optimizing groups, as shown in Fig. 2.

To further improve potency and pharmaceutical properties of the compounds, different side chains were introduced to explore

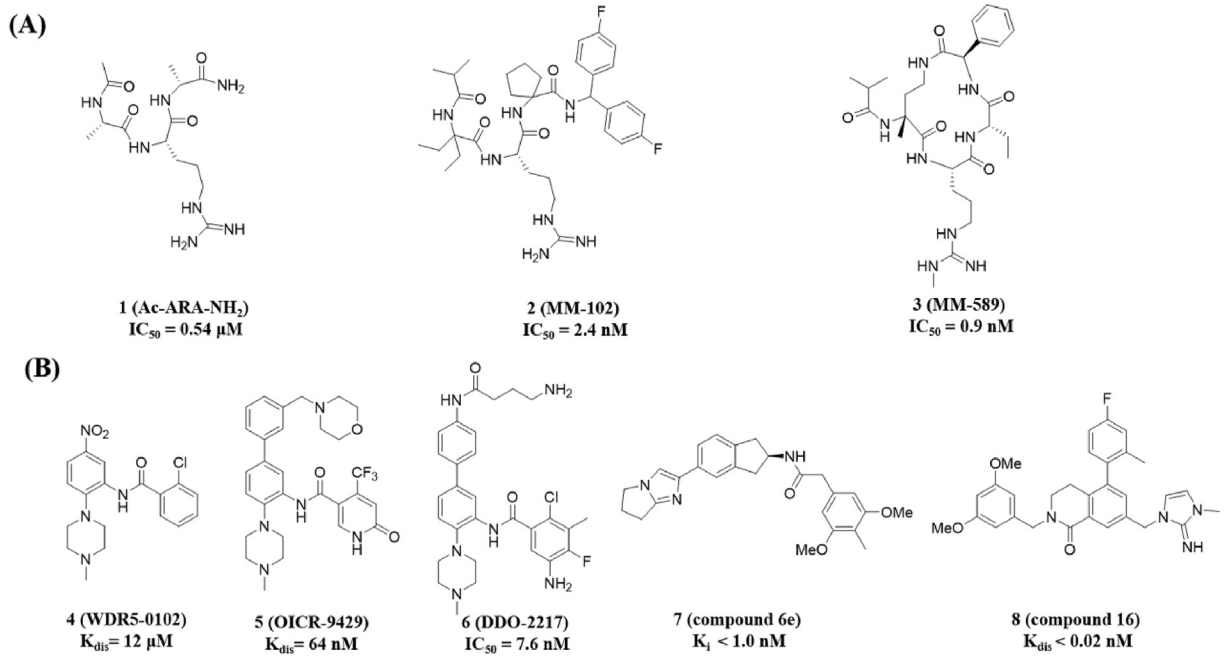

Fig. 1. Chemical structures of previously reported MLL1-WDR5 interaction inhibitors. (A) Peptidomimetics. (B) Small molecular inhibitors.

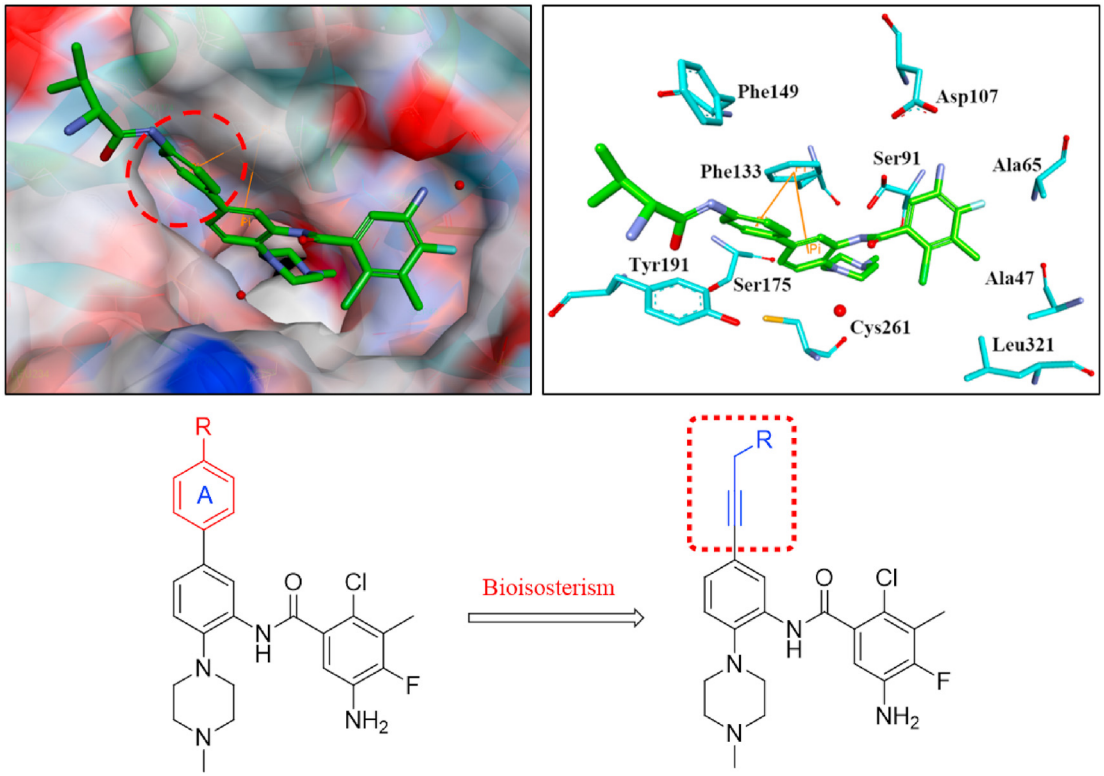

Fig. 2. Structure-based bioisosterism approach to design the series of phenylalkynyl compounds.

solvent regions. The binding affinities of the compounds to WDR5 were evaluated using a fluorescence polarization assay (FP) [28−30,34]. As shown in Table 1, the structure-activity relationship (SAR) of the side chains was consistent with the previously described series of biphenyl compounds [28]. Compared to **9**, it is apparent that the introduction of hydrophilic groups at the amino position exposed to the solvent area enhanced the binding affinity (**9** *vs* **10-15**). Unfortunately, the binding data showed that the phenylalkynyl series compounds resulted in a decline of the binding affinity by approximately 10-fold compared to biphenyl compounds. To explain the decline in activity, we compared the binding models of compound **6** and **10** with the WDR5 binding pocket (Figure S1). The binding models clearly showed that the linear phenylalkynyl structure could open the pocket surrounded by Phe133, Phe149 and Tyr191. However, the smaller alkynyl group could not completely occupy the hydrophobic pocket due to the lack of a π-π stacking interaction with Tyr191 or Phe133. Thus, we next introduced phenyl substituents with hydrophilic groups at this position, yielding **16** and **17**. Indeed, compound **16** and **17** were more potent than compound **10.** The results suggested that the π-π stacking interaction was important for the binding activity.

2.2. Conversion of the phenylalkynyl scaffold to the phenyltriazole structure by click chemistry to improve the activity and drug-like properties

The decline of the binding affinity to WDR5 protein with phenylalkynyl scaffold compounds implied that the linear structure and π-π stacking interaction were important to maintain the potency (Fig. 3). Hence, we designed phenyltriazole scaffold compounds for the following reasons: (1) the phenyltrizole scaffold compounds could be prepared from alkyne and azide by click chemistry, (2) the phenyltriazole structure retained the linear structure, (3) the triazole structure may reform the necessary π-π stacking interaction with Phe133 or Tyr191, and (4) introduction of the triazole structure may further optimize the physicochemical properties [35,36]. On the basis of previous SAR studies, compounds **18-26** with different hydrophilic amino side chains were designed and synthesized. The biphenyl compounds **27-32** with the same side chains as those of the phenyltriazole compounds were designed as control.

The binding affinities to WDR5 and cell antiproliferation properties of these two series of compounds were summarized in Table 2 and Table 3, respectively. As shown in Tables 2 and 3, almost all of these compounds exhibited high binding affinity and cell antiproliferation properties against MV4-11(harboring MLL-AF4 fusion protein) and MOLM-13 (harboring MLL-AF9 fusion protein), which were similar to those of the biphenyl scaffold compounds. Notably, compound **18** is ~10 fold less potent in the FP assay but equipotent in the cellular assay which may due to its high cell-permeability (Table 4). At the same time, these phenyltriazole compounds showed selectivity for HUVEC (non-cancerous human cell line) with low cell toxicity. The introduction of amino side chains significantly increased the binding affinity. The docking study of compound **24** to WDR5 protein supported our hypothesis that the larger sized triazole group may form a π-π stacking interaction with Phe133 and match hydrophobic pocket P_3. In addition, the previously reported key binding interaction elements of biphenyl compounds also contributed greatly to the overall binding affinity of compound **24** (Fig. 4) [28]. The core phenyl ring occupied the P_2 pocket and formed a π-π stacking interaction with Phe133. The amide proton and the carbonyl of the benzamide core formed a direct H-bond interaction with Ser91 residue and a water-bridged interaction with the backbone nitrogen of Cys261 residue, respectively. The *N*-methylpiperazine moiety was positioned deeply in the bottom of P_1 pocket to engage a water-mediated

Table 1
Chemical structures and binding affinities to WDR5 of **9**–**17**.

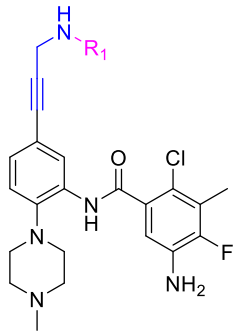

Compd.	R_1	IC_{50}/nM (FP)[a]	Compd.	R_1	IC_{50}/nM (FP)[a]
9	-H	443.8 ± 50.3	**14**	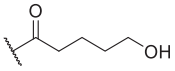	147.9 ± 6.7
10		95.3 ± 10.8	**15**		390.2 ± 12.2
11	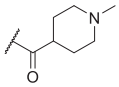	93.5 ± 7.0	**16**	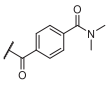	59.7 ± 8.8
12	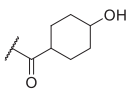	125.0 ± 11.4	**17**	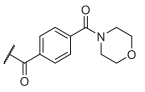	41.0 ± 0.8
13	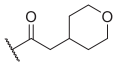	179.4 ± 1.9	–	–	–

[a] Data are expressed as the mean ± SD.

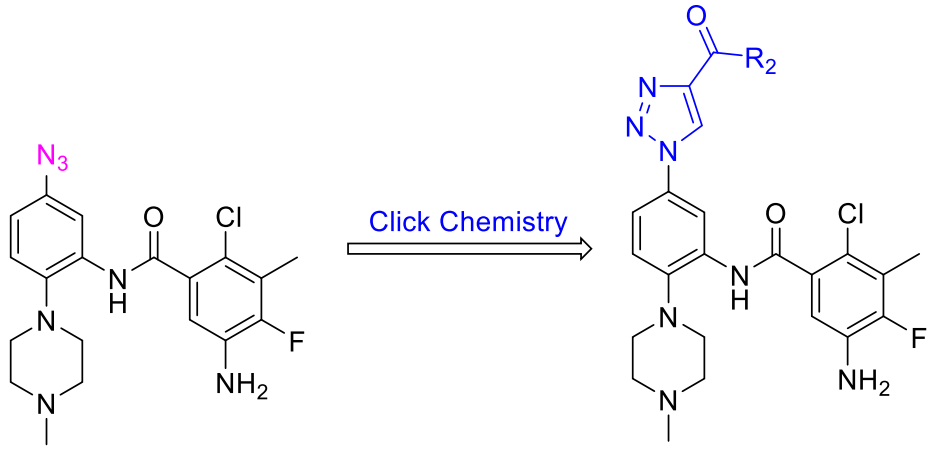

Fig. 3. Click chemistry approach to obtain phenyltriazole compounds.

hydrogen bond with the backbone carbonyl of Cys261. The 2-chloro-3-methyl-4-fluoro-5-aminophenyl occupied the hydrophobic P_4 pocket and an additional H-bond was also identified between the amino proton and Asp107 residue.

2.3. Characterization in biophysical assay and further assessment of selectivity

An isothermal titration calorimetry (ITC) assay was applied to quantify the direct binding of the representative compound, which is commonly employed to assess the thermodynamics and affinity of a ligand-receptor interaction [37]. The resulting ITC profile showed a 1:1 binding stoichiometry, suggesting that one small

Table 2
Chemical structures and binding affinities of **6** and **18**-**32**.

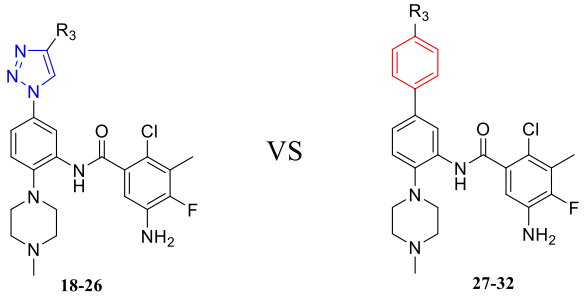

Compd.	R_3	IC_{50}/ nM (FP)[a]	Compd.	R_3	IC_{50}/ nM (FP)[a]
18	-$COOCH_3$	67.8 ± 2.1	**27**	-$COOCH_3$	70.0 ± 2.4
19	-COOH	1036 ± 17.6	**28**	-COOH	98.8 ± 7.3
20		33.9 ± 1.3	**29**		73.0 ± 5.9
21		11.2 ± 1.1	**30**		55.6 ± 6.1
22		15.7 ± 0.5	**31**		15.8 ± 0.3
23	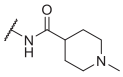	8.9 ± 0.4	**32**	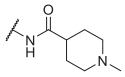	6.5 ± 0.1
24	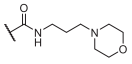	8.6 ± 1.3	**6**	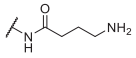	7.6 ± 0.1
25	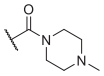	9.0 ± 0.1	-	-	-
26	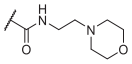	20.4 ± 0.2	-	-	-

[a] Data are expressed as the mean ± SD.

Table 3
The cell antiproliferation activities of **6** and **18**-**32**.

Compd.	IC_{50}/μM (MV4-11)[a] MLL-AF4	IC_{50}/μM (MOLM-13)[a] MLL-AF9	IC_{50}/μM (HUVEC)[a]	Compd.	IC_{50}/μM (MV4-11)[a] MLL-AF4	IC_{50}/μM (MOLM-13)[a] MLL-AF9	IC_{50}/μM (HUVEC)[a]
18	8.9 ± 0.3	11.8 ± 0.9	ND[b]	**26**	17.4 ± 2.1	15.3 ± 0.8	ND[b]
21	10.5 ± 2.0	13.8 ± 1.4	>100	**27**	10.4 ± 0.7	14.8 ± 0.6	ND[b]
22	15.1 ± 1.2	13.2 ± 0.6	>100	**30**	12.5 ± 0.6	10.3 ± 0.7	>100
23	10.9 ± 0.2	8.2 ± 0.6	>100	**31**	10.2 ± 0.9	9.2 ± 1.0	>100
24	8.0 ± 1.2	9.9 ± 1.9	>100	**32**	11.4 ± 0.8	12.5 ± 0.3	>100
25	17.8 ± 3.6	11.9 ± 1.5	ND[b]	**6**	7.4 ± 1.4	ND[b]	>100

[a] Data are expressed as the mean ± SD.
[b] ND = not determined.

Table 4
Physicochemical properties of the series of phenyltriazole and biphenyl compounds.

Compd.	$P_e/10^{-6}$ cm/s (pH = 7.4)[a]	Solubility/μmol/L (pH = 7.4)	Compd.	$P_e/10^{-6}$ cm/s (pH = 7.4)[a]	Solubility/μmol/L (pH = 7.4)
18	63.6 ± 5.1	41.5	**27**	48.3 ± 3.2	3.7
19	4.0 ± 0.4	348.9	**28**	7.3 ± 1.4	40.5
21	64.5 ± 4.8	360.9	**30**	47.7 ± 3.2	48.2
22	44.6 ± 2.8	95.6	**31**	50.9 ± 5.3	3.9
23	17.8 ± 1.3	343.4	**32**	3.9 ± 0.8	126.4
24	17.2 ± 4.8	245.9	**6**	1.6 ± 0.2	199.1

[a] Data are expressed as the mean ± SD.

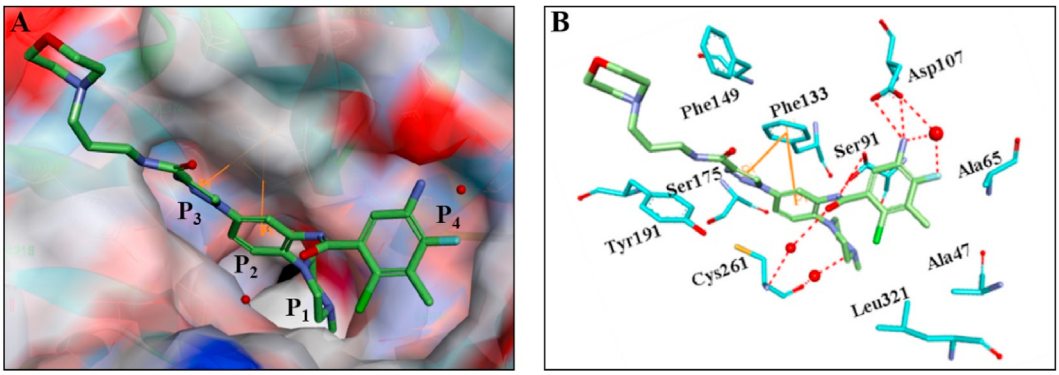

Fig. 4. The docking study of compound **24** to WDR5 protein (PDB code: 4IA9). (A) Compound **24** inserts into the active site of WDR5, with the surface colored in terms of the charge state. (B) The detailed interactions between WDR5 and compound **24**. The carbon atoms of compound **24** and WDR5 residues are colored light green and light blue, respectively. Hydrogen bonds are represented as red dashed lines, and the π-π stacking interaction are displayed with orange lines.

molecule bound to one molecule of WDR5. The curve-fitting analysis of parameters indicated that **24** had a K_d value of 11.6 nM. Both a strong enthalpic change ($\Delta H = -10.2 \pm 0.2$ kcal·mol^{-1}) and a favorable entropy change ($-T\Delta S = -0.629$ kcal·mol^{-1}) contributed to Gibbs free energy, which suggested a synergistic enthalpy/entropy-driven process in the binding of compound **24** to WDR5 (Fig. 5A and B).

We next examined **24** inhibitory activity not only on the MLL1 HMT activity (H3K4 enzyme), but also toward four histone lysine methyltransferases and an arginine methyltransferase. We were pleased to find that compound **24** is specific for the MLL1 HMTase, and did not affect G9a (H3K9), DOT1L (H3K79), EZH2 (H3K27), SET8 (H4K20) and PRMT5 within the tested concentration range (Fig. 5C). Collectively, compound **24** tightly and directly bound to the WDR5 protein and then selectively inhibited MLL complex HMT Activity *in vitro*.

In an effort to further identify potential druglike compounds, we next evaluated the physicochemical properties of the representative compounds. The intrinsic aqueous solubility was determined on a Gemini Profiler instrument (*p*ION) by the "gold standard" Avdeef-Bucher potentiometric titration method [38,39]. The permeability is also an important property reflecting the ability of molecules to diffuse through the cell membrane. We determined the permeability of the derivatives by using the PAMPA Explorer instrument (*p*ION). The data showed that the phenyltriazole compounds displayed satisfactory permeability (P_e = 16-64 × 10^{-6} cm/s, pH = 7.4). Notably, these compounds showed significantly improved aqueous solubility (Table 4). The observations proved that the optimization of the phenyltriazole scaffold efficiently improved the physicochemical properties, especially the solubility. Taken together, compound **24** demonstrated the most potent binding affinity and cell viability as well as proper solubility and permeability, and as a result, it was selected for further pharmacological evaluation both *in vitro* and *in vivo*.

2.4. Compound 24 inhibited MLL complex HMT activity and downstream gene expression in MV4-11 cells

MLL1-WDR5 interaction is required for the MLL complex to achieve its H3K4 HMT activity [2,40,41]. The MLL1-WDR5 interaction inhibitor may effectively inhibit the MLL HMT activity. Therefore, compound **24** was characterized for its inhibition of the MLL HMT activity in MV4-11 cells. Our previously reported **DDO-2084** was selected as a positive control (Fig. 6A) [28]. As shown in Fig. 6B, compound **24** could dose-dependently reduce the mono-, di-, and trimethylation of H3K4. The methylation of H3K4 was essential for the activation of downstream gene expressions [42–44]. Corresponding to the change in H3K4me, the expression of MLL1 target gene *HOXA9* and cofactor *Meis1* was significantly decreased compared to the DMSO control (Fig. 6C). Approximately 60% and

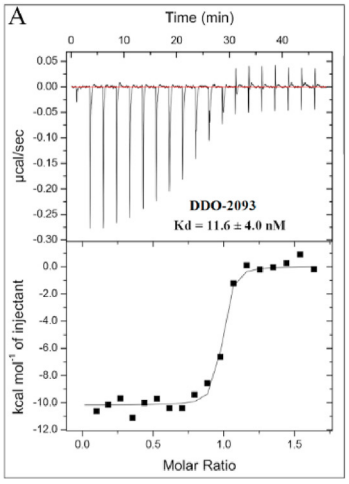

B

N	K_d (nM)	ΔH kcal·mol^{-1}	-TΔS kcal·mol^{-1}	ΔG kcal·mol^{-1}
0.95 ± 0.008	11.6 ± 4.0	-10.2 ± 0.2	-0.63	-10.83

C

Compd. 24	MLL1 (H3K4)	G9a (H3K9)	DOT1L (H3K79)	EZH2 (H3K27)	SET8 (H4K20)	PRMT5 (H3R8/H4R3)
IC_{50}(μM)	0.174	>100	>100	>100	>100	>100

Fig. 5. Binding affinity of **24** evaluated with the ITC. (A) The heat of binding plotted versus time (upper panels) and the curve-fitting of the binding model (lower panels). (B) The binding parameters of the ITC assay. (C) The selectivity of compound **24** to HMT activity of reconstituted MLL1 core complex over other Methyltransferases *in vitro*.

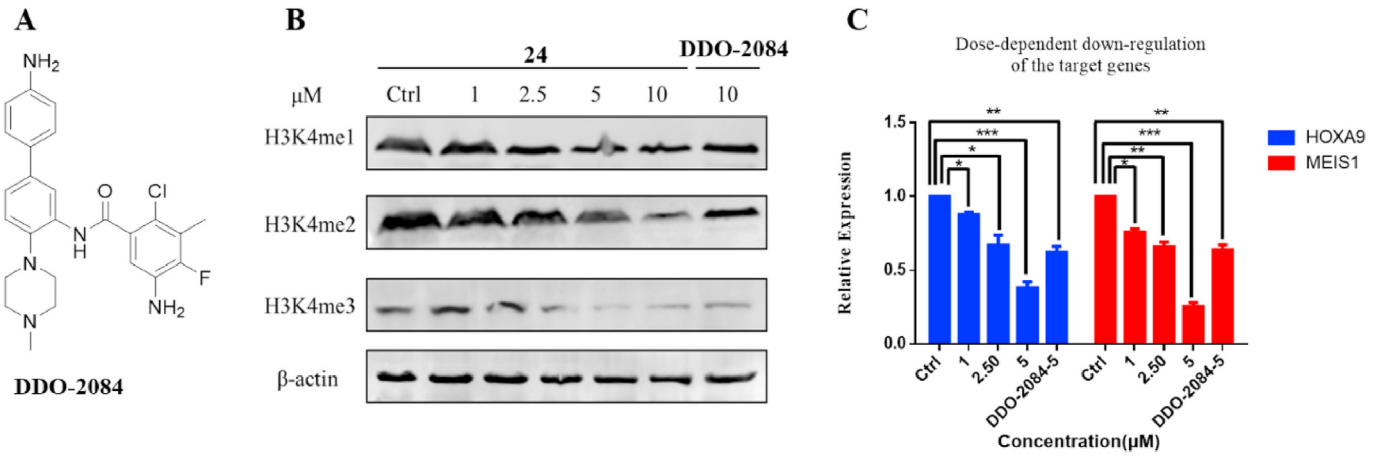

Fig. 6. Structure of positive control compound **DDO-2084,** and compound **24** specifically inhibited H3K4me and downstream gene expression. (A) Structure of **DDO-2084**. (B) Western blot analysis for the inhibition of H3K4me activity after treatment of MV4-11 cells with DMSO and various concentrations (1, 2.5, 5, and 10 μM) of compound **24**. (C) The inhibition of *HOXA9* and *Meis1* gene expressions in MV4-11 cells after treatment with different concentrations (0, 1, 2.5, and 5 μM) of compound **24** assessed by RT-PCR. The values shown are the mean ± SD (n = 3). *p < 0.05, **p < 0.01, ***p < 0.001, indicate a statistically significant difference from the nontreated blank control group.

70% reduction in *HOXA9* and *Meis1* gene expression were observed after treatment of MV4-11 cells with 5 μM of compound **24**, respectively. Disturbing the MLL1-WDR5 interaction with our compound **24** could efficiently reduce the H3K4me activity and MLL-fusion protein dependent genes expression.

2.5. In vivo antitumor efficacy of compound 24

On the basis of the favorable *in vitro* activity for compound **24,** it was chosen to investigate the preliminary anticancer efficacy *in vivo*. In this study, a MV4-11 xenograft model was established to evaluate its antitumor growth activity. When tumors had reached an average volume of 100 mm^3, three doses of 20 mg/kg, 40 mg/kg and 80 mg/kg of **24** were administered intraperitoneally (*i.p.*) to mice for 21 consecutive days, respectively. Cytarabine (ARAC) (100 mg/kg) was chosen as the reference, which is a chemotherapy agent mainly used in the treatment of acute myeloid leukemia (AML) [45]. The tumor growth and body weight were measured and recorded. Compound **24** significantly suppressed the tumor size and weight in a dose-dependent manner (Fig. 7). Compared to the control group, the tumor volume growth inhibition (GI) values for groups treated with **24** were calculated to be 13.7%, 37.6% and 63.9% with doses of 20 mg/kg, 40 mg/kg and 80 mg/kg, respectively (Fig. 7A). The 80 mg/kg treatment groups caused a 60.0% TGI (The tumor weight growth inhibition) (Fig. 7C). The TGI in the 80 mg/kg group of **24** was equal to that of the 100 mg/kg group of ARAC. Notably, no obvious changes were observed in the behavior and body weight of mice during treatment with **24** (Fig. 7B). The results highlighted that compound **24** exhibited *in vivo* antitumor effects.

To determine whether the tumor growth inhibition by compound **24** was due to blocking the MLL1-WDR5 interaction and repressing their special mechanism of action, we harvested tumor tissue after drug treatments and evaluated the HMT activity by Western blot as well as downstream signaling gene expression by RT-PCR (Fig. 8). Consistent with the pharmacodynamic biomarker changes *in vitro*, compound **24** could dose-dependently reduce the H3K4me levels and significantly decrease the expression of the target *HOXA9* and *Meis1* genes *in vivo*. Overall, *in vivo* experimental data validated that **24** could suppress MLL1 HMT catalyzed function, decrease the leukemia signaling molecules and thereby inhibit tumor growth.

2.6. Safety evaluation of compound 24

To evaluate the *in vivo* safety of compound **24**, mice subacute toxicity experiments were carried out. As shown in Fig. 8, no apparent signs associated with animal toxicity were observed during the treatment period of *ip*-administered normal mice treated with **24** at 80, 200, and 300 mg/kg every day for 14 days. Compared to the control group, the body weights of the treatment groups increased gradually. No behavioral abnormalities were observed, and the organ/body weight ratios of the heart, liver, spleen, lungs, and kidneys also did not change after the administration of **24** (Fig. 9). The hematoxylin-eosin (HE) staining of organs showed no obvious tissue damage in normal mice under the high-dose administration of **24** (Fig. 10). Thus, compound **24** may have a wide therapeutic window.

2.7. Chemistry

The synthesis of target compounds **9-17** was summarized in Scheme 1. Briefly, intermediate **34** was prepared from commercial propargylamine via *t*-butyloxycarboryl group protection. Then, the Sonogashira reaction was conducted in the presence of bis-triphenylphosphine palladium dichloride and cuprous iodide to produce the key intermediate **35**. The fluoro group of **35** was substituted with *N*-methylpiperazine affording **36**, followed by reducing intermediate **36** with stannous chloride to obtain **37**. Intermediate **37** was condensed with previously obtained 2-chloro-3-methyl-4-fluoro-5-nitrobenzoyl chloride **54** to give intermediate benzamide **38**. Subsequently, nitro intermediate **38** was reduced and simultaneously deprotected with stannous chloride to get target compound **9**. Finally, compound **9** was acylated with different acids and catalyzed by Castro's reagent to yield **10-17.**

Compounds **18-26** were prepared by following the procedures described in Scheme 2. Briefly, 4-fluoro-3-nitroaniline **39** was substituted with *N*-methylpiperazine producing intermediate **40**. Intermediate **41** was prepared by the reactions of diazotization and azide and then cyclized via click chemistry with methyl propionate in the presence of cuprous iodide to get key intermediate **42**. Target compound **18** was afforded by the reactions of reduction, condensation and reduction described in Scheme 2. Compound **19** was obtained by hydrolyzing the methyl ester. Compound **19** was condensed with different amines to give target compounds **20-26**.

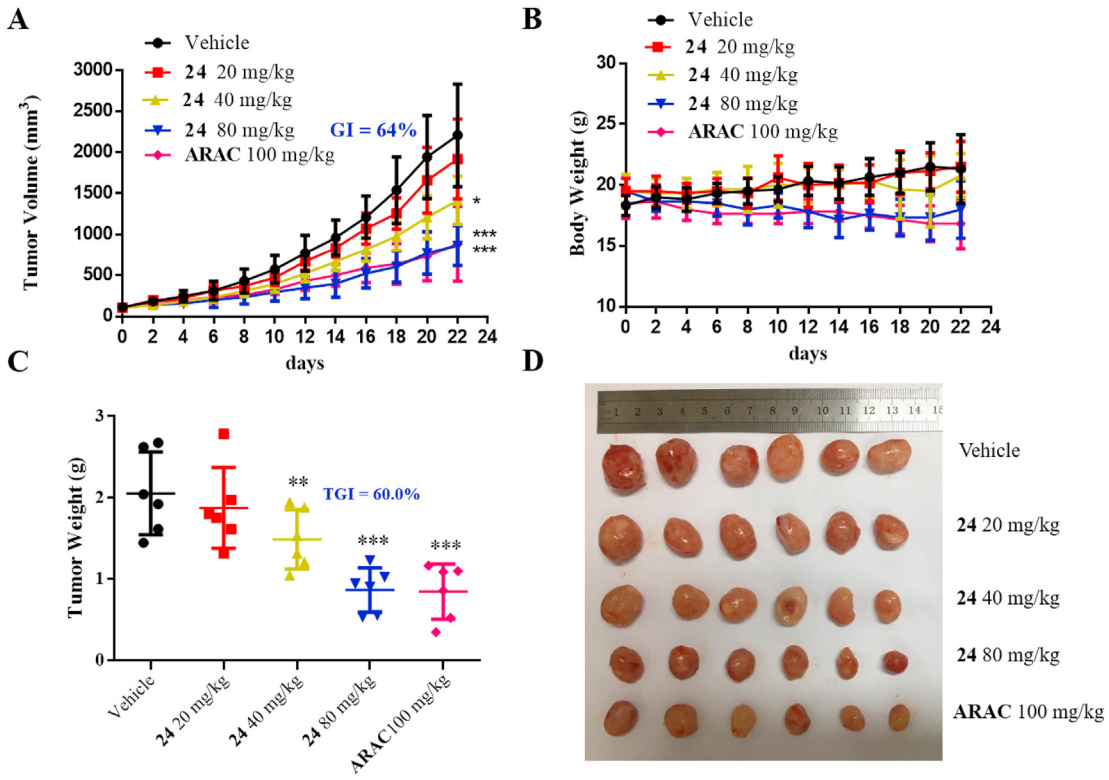

Fig. 7. Antitumor efficacy of compound **24** in MV4-11 human leukemia cancer xenografts. (A) Growth difference of tumor volumes, with the GI being the tumor volume growth inhibition. (B) Mice body weight. (C) At the end of experiment, tumors were resected and weighed. The black lines indicated the average value of the tumor weights. The TGI was the tumor weight growth inhibition. *p < 0.05, **p < 0.01, ***p < 0.001, indicate a statistically significant difference from the nontreated control group. (D) Images of the excised tumors for each group.

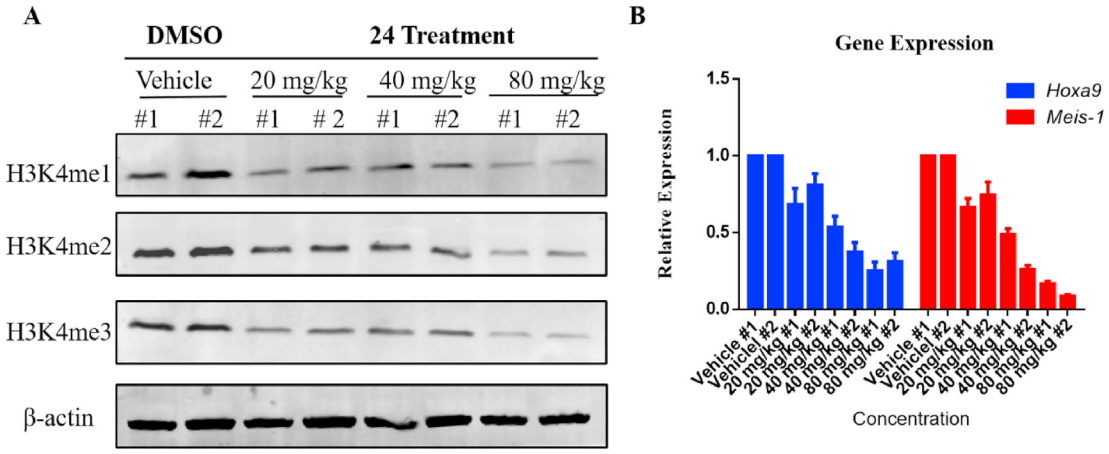

Fig. 8. Pharmacodynamic biomarker changes in tumor xenografts. (A) Western blot analysis of the H3K4me activity. (B) The target gene expressions examined by RT-PCR.

We previously developed an efficient synthetic route for preparing compound **6**, which allows compound **31** and **32** to be installed at the last step of the synthetic sequence [28]. The detailed synthetic route can also be found in the supporting information (Scheme S1). We also inverted the amide bond to introduce various side chains. Using a similar synthetic route, we obtained **27-30** (Scheme 3).

3. Conclusions

In the present study, we analyzed the binding mode of small molecular inhibitors to WDR5 protein. The binding information displayed that the linear skeleton and the hydrophobic interaction between ring A of biphenyl compounds and the WDR5 binding pocket formed by Phe133, Phe149 and Tyr191 were important to maintain the binding affinity. Hence, we applied a linear scaffold hopping to discover novel phenylalkynyl inhibitors by keeping the linear structure and reducing the rigidity of the molecules. Although both their binding affinities and cell potency decreased, the alkynyl structure provided the basis for the synthesis of a series of phenyltriazole compounds by click chemistry. As expected, almost all of the phenytriazole scaffold compounds displayed equal

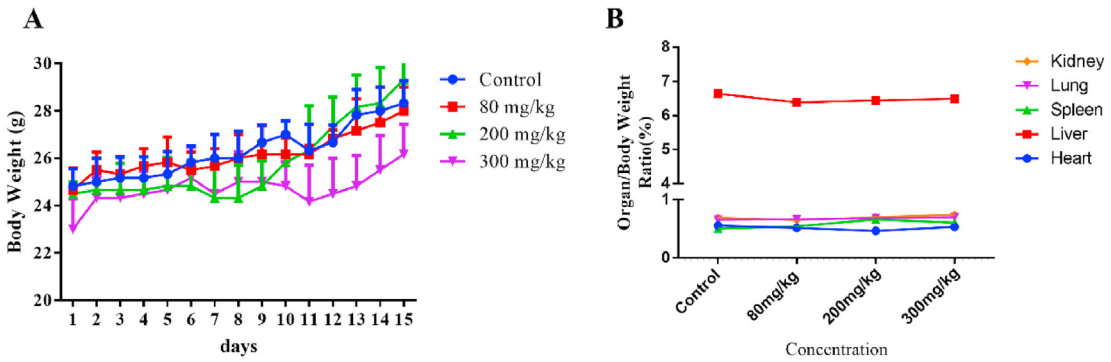

Fig. 9. The effect of *ip*-administered 80, 200, and 300 mg/kg of **24** on the body weight and organ/body weight ratios of normal mice (A) body weight change, (B) organ/body weight ratio change of the heart, liver, spleen, lungs and kidneys.

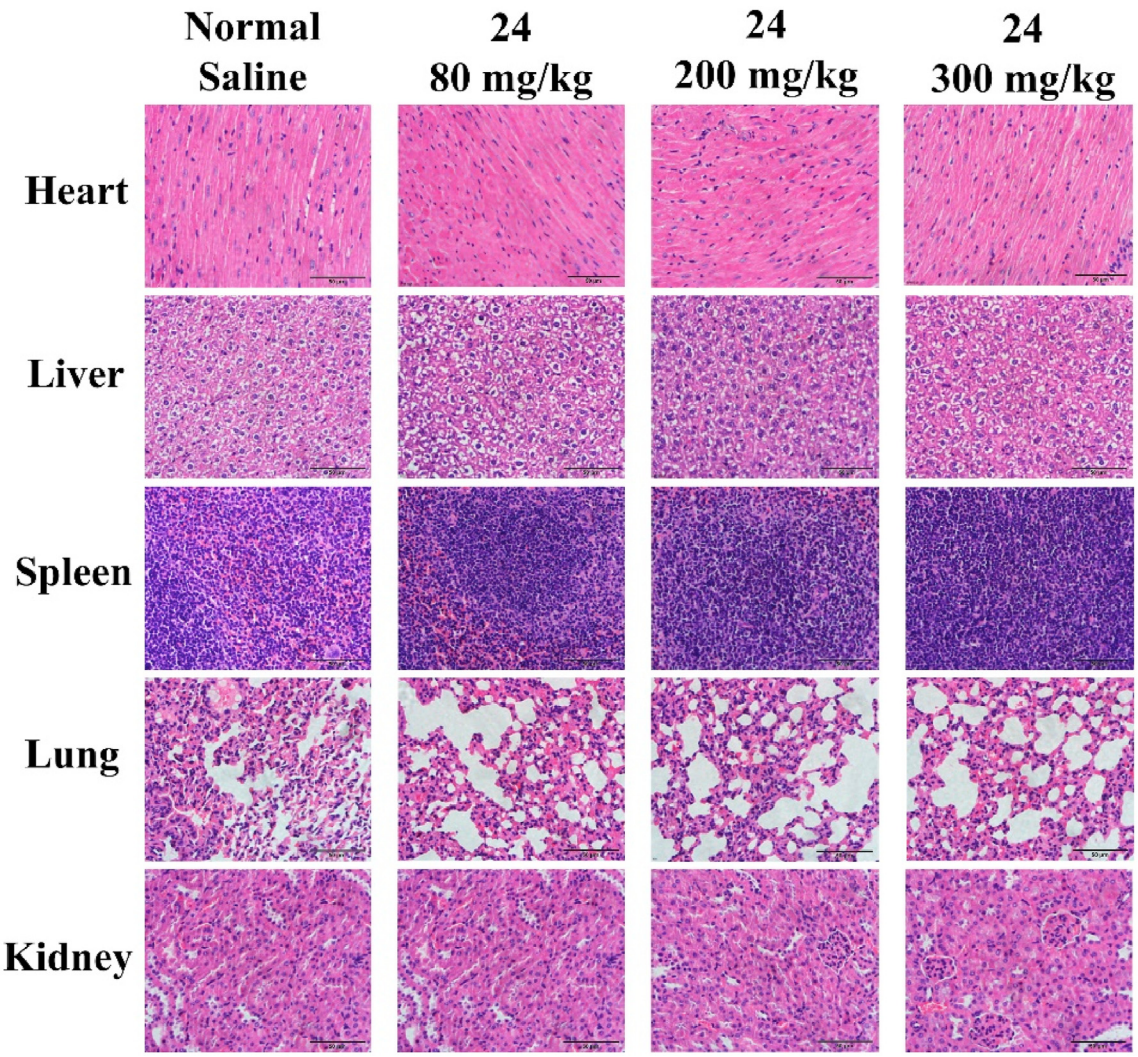

Fig. 10. Representative images of heart, liver, spleen, lung and kidney tissues stained by hematoxylin and eosin. First row: normal saline. Second row: administration of 80 mg/kg of **24.** Third row: administration of 200 mg/kg of **24**. Fourth row: administration of 300 mg/kg **24.** Scale bars represent 50 μm.

in vitro potency and significantly improved physicochemical properties compared to the biphenyl compounds. Among them, compound **24 (DDO-2093)** exhibited the most potent binding affinity with an IC_{50} value of 8.6 ± 1.3 nM determined by the FP assay and a K_d value of 11.6 ± 4.0 nM examined by the ITC assay. Moreover, **24** selectively inhibited the catalytic activity of MLL complex *in vitro*. Meanwhile, compound **24** also displayed obvious antiproliferative activities against two human acute leukemia cell lines with IC_{50} values of 8.0 ± 1.2 μM and 9.9 ± 1.9 μM, respectively and showed high selectivity for non-cancerous human cell line

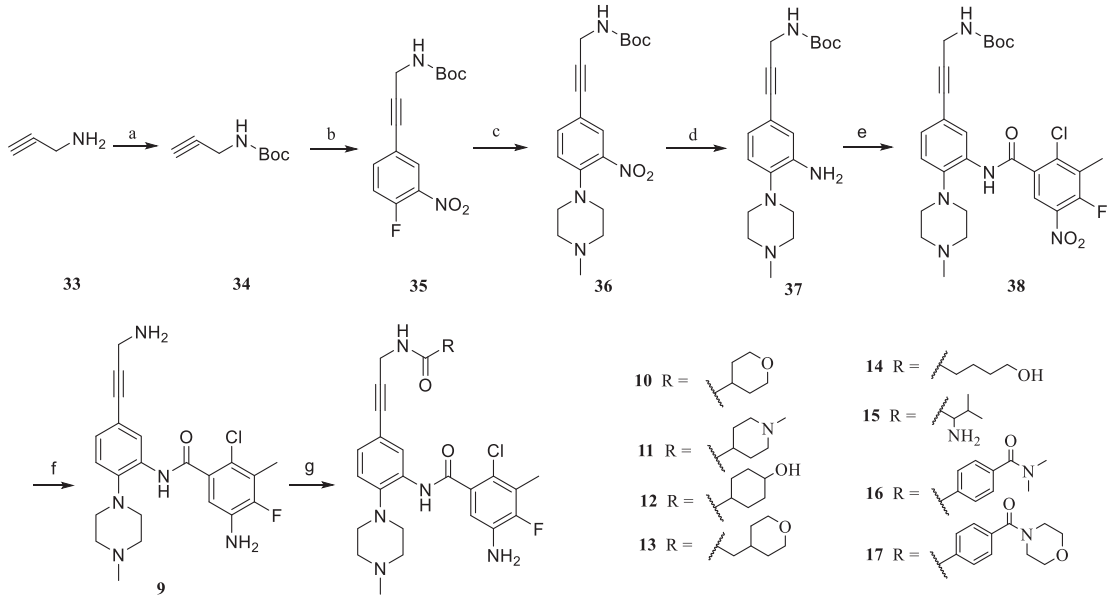

Scheme 1. Synthetic Route of Phenylalkynyl Compounds 9-17[a]

[a]Reagents and Conditions: (a) Boc_2O, DCM, r.t. 1 h; (b) 1-fluoro-4-iodo-2-nitrobenzene, $Pd(PPh_3)_2Cl_2$, CuI, TEA, CH_3CN, r.t., 1 h; (c) 1-methylpiperazine, DIPEA, DMF, r.t., 2 h; (d) $SnCl_2.2H_2O$ (5 equiv), EA, reflux, 4 h; (e) 2-chloro-4-fluoro-3-methyl-5-nitrobenzoyl chloride (**54**), pyridine, DCM, r.t., 6 h; (f) $SnCl_2 \cdot 2H_2O$ (10 equiv), EA, reflux, 3 h; (g) different acids, BOP, TEA, DMF, r.t., 4–8 h.

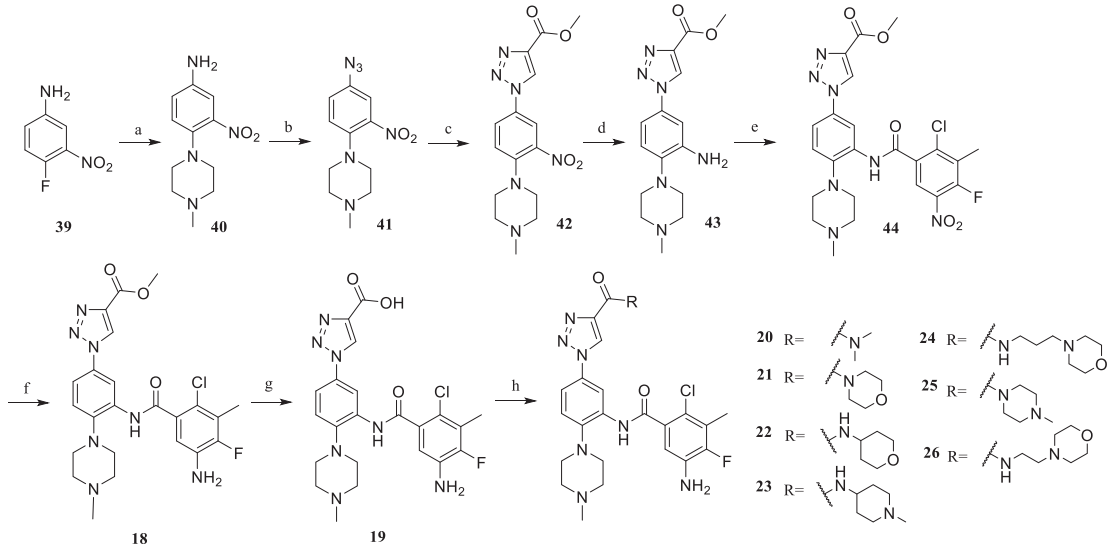

Scheme 2. Synthesis of Phenyltriazole Compounds **18**-**26**[a]

[a] Reagents and Conditions: (a) 1-methylpiperazine, DIPEA, CH_3CN, reflux, 12 h; (b) (i) $NaNO_2$, 6 M/HCl, 0 °C, 0.5 h; (ii) NaN_3, 0 °C, 0.5 h, then r.t., 2 h; (c) methyl propiolate, CuI, MeOH, DIPEA, reflux, 48 h; (d) H_2, Pd/C, MeOH, r.t., 6 h; (e) 2-chloro-4-fluoro-3-methyl-5-nitrobenzoyl chloride (**54**), pyridine, DCM, r.t., 6 h; (f) $SnCl_2.2H_2O$ (5 equiv), EA, reflux, 3 h; (g) 1 M/LiOH, THF, r.t., overnight; (h) amines, BOP, TEA, DMF, r.t., 4–8 h.

(IC_{50} > 100 μM). Notably, compound **24** showed balanced aqueous solubility and permeability, which make it suitable for further pharmacodynamic evaluation *in vivo*. Experiments with subcutaneously implanted MV4-11 xenografts indicated that treatment with **24** resulted in a significant reduction in the tumor volume compared with the control group, with a 63.9% tumor volume reduction observed at the dose of 80 mg/kg/day (ip). Furthermore, the mechanistic studies validated that compound **24** could also repress MLL1 HMT activity and downstream signaling gene expression in cells and *in vivo*, emphasizing that compound **24** was on-target. Furthermore, **24** had a large therapeutic window with no apparent toxicity observed in normal mice. These results first verified that using small molecular inhibitors to block the MLL1-WDR5 PPI may be a feasible approach for treating MLL fusion leukemia. Taken together, the phenyltriazole scaffold derivative **24** was a valuable tool for the biomedical community to investigate the role of the MLL1-WDR5 PPI.

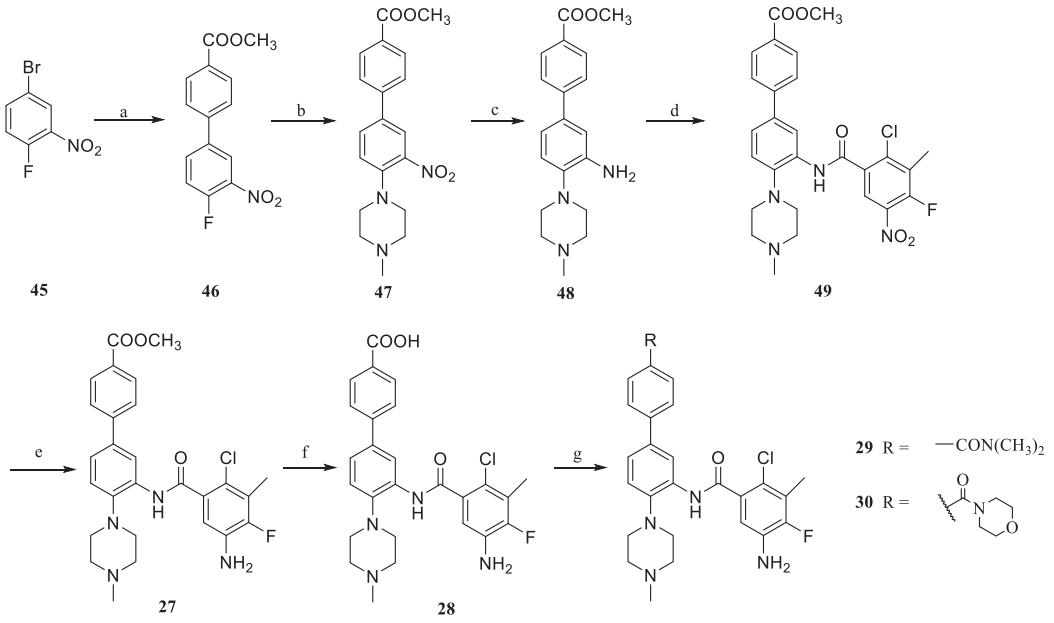

Scheme 3. Synthesis of the Designed Biphenyl Compounds **27**-**30**[a]

[a] Reagents and Conditions: (a) methyl 4-boronobenzoate, $Pd(PPh_3)_2Cl_2$, Cs_2CO_3, dioxane, reflux, 8 h; (b) *N*-methyl piperazine, DIPEA, DMF, 80 °C, 4 h; (c) $SnCl_2$, ethyl acetate, reflux, 6 h; (d) 2-chloro-4-fluoro-3-methyl-5-nitrobenzoyl chloride, pyridine, DCM, r.t, 4 h; (e) $SnCl_2$, ethyl acetate, reflux, 6 h; (f) 1 M LiOH, THF, r.t., 2 h; (g) different amines, BOP, TEA, DMF, r.t, 6—10 h.

4. Experiments section

4.1. Chemistry

General information. All reagents and solvents were obtained from commercial vendors. Organic solvents were reagent grade and, when necessary, were purified and dried according to standard procedures. Air and/or moisture sensitive reactions were performed under nitrogen. Solvent removal from reaction mixtures was carried out by rotary evaporation under reduced pressure. The yields given refer to chromatographically purified compounds unless stated otherwise. Reactions were monitored by thin-layer chromatography (TLC) on 0.25 mm silica gel plates (GF254) and visualized under UV light at 254 and 365 nm. Melting points were determined with a Mel-TEMP II apparatus. The ^{1}H NMR spectras were determined with a Bruker AV-300 instrument using deuterated solvents with tetramethylsilane (TMS) as internal standard. EI-MS was collected on shimadzu GCMS-2010 instruments. ESI-mass and high resolution mass spectra (HRMS) were recorded on a Water Q-Tof micro mass spectrometer. The purity (≥95%) of the compounds was verified by the HPLC study performed on an Agilent C18 (4.6 mm × 150 mm, 3.5 μM) column using a mixture of solvent methanol/water at a flow rate of 0.5 mL/min and monitored by UV absorption at 254 nm.

4.1.1. 5-amino-N-(5-(3-aminoprop-1-yn-1-yl)-2-(4-methylpiperazin-1-yl) phenyl)-2-chloro-4-fluoro-3-methylbenzamide ***(9)***

To a solution of **38** (0.7 g, 1.2 mmol) in EA (80 mL) at room temperature was added $SnCl_2.2H_2O$ (2.8 g, 12.5 mmol). The resulting solution was then refluxed with vigorous stirring for 3 h, and subsequently cooled to room temperature. Following dilution with EA (100 mL) and the mixture was neutralized with saturated sodium bicarbonate solution. Then filtered and washed residue with EA (5 × 40 mL), and the organic phase was separated and dried (Na_2SO_4), filtered, and concentrated. The residue was washed with EA to afford grey white solid **9** (0.42 g). ^{1}H NMR (300 MHz, DMSO-d_6) δ 9.28 (s, 1H), 8.04 (s, 1H), 7.17 (s, 2H), 6.84 (d, J = 9.3 Hz, 1H), 5.51 (s, 2H), 3.50 (s, 2H), 2.86 (t, J = 4.6 Hz, 4H), 2.44 (br s, 4H), 2.25 (d, J = 2.7 Hz, 3H), 2.20 (s, 3H), 1.23 (s, 2H). ^{13}C NMR (75 MHz, DMSO-d_6) δ 164.90, 150.74, 147.55, 143.52, 135.57, 132.39, 132.04, 127.72, 124.49, 123.30, 123.08, 120.57, 119.47, 118.21, 112.77, 91.46, 80.97, 54.76, 54.53, 51.11, 50.51, 45.69, 31.29, 24.57, 11.96. HRMS (ESI): calcd. for *m/z* $C_{22}H_{26}ClFN_5O$ $[M + H]^+$ 430.1804, found. 430.1826. HPLC (80% methanol in water): t_R = 4.018 min. 97.75%. Yield: 77.8%. m.p. > 250 °C.

4.1.1.1. Tert-butyl prop-2-yn-1-ylcarbamate ***(34)***.

To a solution of prop-2-yn-1-amine (10.0 g, 181.6 mmol) in DCM (100 mL) was added $(Boc)_2O$ (41.6 g, 190.1 mmol) dropwise at 0 °C and stirred for 1 h. Upon completion, the solution was concentrated under reduced pressure, and crystalized at 0 °C. Then the residue was washed by cold petroleum ether to afford white solid (20.3 g). Yield: 71.9%

4.1.1.2. Tert-butyl (3-(4-fluoro-3-nitrophenyl) prop-2-yn-1-yl) carbamate ***(35)***.

A mixture of 1-fluoro-4-iodo-2-nitrobenzene (4.4 g, 16.5 mmol), $Pd(PPh_3)_2Cl_2$ (0.58 g, 0.82 mmol), CuI (0.16 g, 0.82 mmol), and *tert*-butyl prop-2-yn-1-ylcarbamate **34** (5.1 g, 33.0 mmol) was dissolved in 10 mL of Et_3N and 100 mL of CH_3CN. The reaction mixture was stirred at room temperature for 1 h. The solvent was removed under reduced pressure, and the residue was purified by silica gel column chromatography (petroleumether/EA) (40:1 to 10:1 v/v) to give compound **35** as light yellow solid (3.6 g). ^{1}H NMR (300 MHz, DMSO-d_6) δ 8.03 (dd, J = 7.2, 2.2 Hz, 1H), 7.77—7.73 (m, 1H), 7.55—7.48 (m, 1H), 7.31 (s, 1H), 3.91 (d, J = 5.7 Hz, 2H), 1.31 (s, 9H). *m/z* (EI-MS): 317.1 $[M + Na]^+$. Yield: 74.1% m.p. 86—89 °C.

4.1.1.3. .***Tert-butyl (3-(4-(4-methylpiperazin-1-yl)-3-nitrophenyl) prop-2-yn-1-yl) carba-mate (36)***.

To a solution of compound **35** (3.6 g, 12.2 mmol) in CH_3CN (50 mL) at room temperature was

added *N*-methyl piperazine (2.4 g, 2.6 mL, 24.4 mmol), followed by *N*, *N*-diisopropylethylamine (4.0 mL, 24.4 mmol). Then the resulting solution was stirred at room temperature for 2 h. Following dilution with EA (150 mL), the mixture was washed with water (3 × 50 mL), then the organic phase was dried (Na_2SO_4), filtered, and concentrate to give compound **36** as yellow solid (4.4 g). ^{1}H NMR (300 MHz, DMSO-d_6) δ7.79 (d, J = 2.1 Hz, 1H), 7.54 (dd, J = 8.6, 2.1 Hz, 1H), 7.35 (s, 1H), 7.25 (d, J = 8.7 Hz, 1H), 3.97 (d, J = 5.7 Hz, 2H), 3.02 (t, J = 4.7 Hz, 4H), 2.40 (t, J = 4.8 Hz, 4H), 2.20 (s, 3H), 1.39 (s, 9H). *m/z* (EI-MS): 397.2 $[M + Na]^+$. Yield: 97.8%. m.p. 121–124 °C.

*4.1.1.4. Tert-butyl (3-(3-amino-4-(4-methylpiperazin-1-yl) phenyl) prop-2-yn-1-yl) carba-mate **(37)**.* To a solution of **36** (2.3 g, 6.1 mmol) in EA (100 mL) at room temperature was added $SnCl_2.2H_2O$ (4.2 g, 18.4 mmol). The resulting solution was then refluxed with vigorous stirring for 4 h, and subsequently cooled to room temperature. Following dilution with EA (100 mL) and the mixture was neutralized with saturated sodium bicarbonate solution. Then filtered and washed residue with EA (5 × 40 mL), and the organic phase was dried (Na_2SO_4), filtered, and concentrated to afford grey white solid **37** (1.7 g). ^{1}H NMR (300 MHz, DMSO-d_6) δ 7.32 (s, 1H), 6.83 (d, J = 7.6 Hz, 1H), 6.70 (s, 1H), 6.59 (d, J = 8.0 Hz, 1H), 4.80 (s, 2H), 3.92 (d, J = 5.7 Hz, 2H), 2.79 (br s, 4H), 2.50 (br s, 4H), 2.22 (s, 3H), 1.40 (s, 9H). *m/z* (EI-MS): 345.2 $[M + H]^+$. Yield: 80.9%. m.p. 205–208 °C.

*4.1.1.5. Tert-butyl (3-(3-(2-chloro-4-fluoro-3-methyl-5-nitrobenzamido)-4-(4-methyl-piperazin-1-yl) phenyl) prop-2-yn-1-yl) carbamate **(38)**.* To a solution of **37** (2.0 g, 5.8 mmol) in anhydrous dichloromethane (100 mL) was added 2-chloro-4-fluoro-3-methylbenzoyl chloride **54** (1.8 g, 7.0 mmol) at 0 °C. This was followed by the addition of pyridine (0.93 mL, 11.6 mmol), and the resulting solution was stirred at room temperature for 6 h. The reaction was subsequently diluted with dichloromethane (50 mL) and washed with w saturated sodium bicarbonate solution (3 × 50 mL), then saturated sodium chloride solution (30 mL). The organic phase was then separated, dried (Na_2SO_4), filtered, and concentrated to provide crude product. Then purified by column chromatography on silica gel using a common 1% MeOH/DCM gradient to afford compound **38** as light yellow solid (2.4 g). ^{1}H NMR (300 MHz, DMSO-d_6) δ 9.76 (s, 1H), 8.31 (d, J = 7.7 Hz, 1H), 7.93 (d, J = 1.9 Hz, 1H), 7.36 (d, J = 6.2 Hz, 1H), 7.27–7.08 (m, 2H), 3.97 (d, J = 5.8 Hz, 2H), 2.91 (t, J = 4.5 Hz, 4H), 2.47 (br s, 4H), 2.42 (d, J = 2.7 Hz, 3H), 2.20 (s, 3H), 1.40 (s, 9H). *m/z* (EI-MS): 560.2 $[M]^+$. Yield: 75.0%. m.p. 151–154 °C.

4.1.2. General procedure for the synthesis of 10–17

To a solution of acid (0.46 mmol) in DMF (10 mL) at room temperature was added BOP reagent (0.12 g, 0.28 mmol), followed by TEA (0.06 mL, 0.46 mmol). The mixture was stirred for 0.5 h before compound **9** (0.1 g, 0.23 mmol) was added. Then the resulting solution was stirred at room temperature for 4–8 h. The aqueous solution was diluted with EA (50 mL) and the mixture was washed with saturated sodium chloride solution (3 × 30 mL). The organic phase was then separated, dried (Na_2SO_4), filtered, and concentrated to provide crude product. Then purified by column chromatography on silica gel using a common 2–5% MeOH/DCM gradient to afford compounds **10-17.**

*4.1.2.1. N-(3-(3-(5-amino-2-chloro-4-fluoro-3-methylbenzamido)-4-(4-methylpiperazi-n-1-yl) phenyl) prop-2-yn-1-yl) tetrahydro-2H-pyran-4-carboxamide **(10)**.* ^{1}H NMR (300 MHz, DMSO-d_6) δ 9.37 (s, 1H), 8.36 (s, 1H), 8.02 (s, 1H), 7.31–7.11 (m, 2H), 6.81 (d, J = 9.2 Hz, 1H), 5.50 (s, 2H), 4.12 (d, J = 5.4 Hz, 2H), 3.87–3.84 (m, 2H), 3.34–3.30 (m, 2H), 3.29–3.25 (m, 1H), 2.98 (br s, 4H), 2.84 (br s, 4H), 2.54 (s, 3H), 2.25 (d, J = 2.6 Hz, 3H), 1.60 (t, J = 6.0 Hz, 4H). HRMS (ESI): calcd. for *m/z* $C_{28}H_{33}ClFN_5O_3$ $[M + H]^+$ 542.2329, found 542.2342. HPLC (80% methanol in water): t_R = 4.859 min, 97.71%. Yield: 53.8%. m.p. 150–153 °C.

*4.1.2.2. N-(3-(3-(5-amino-2-chloro-4-fluoro-3-methylbenzamido)-4-(4-methylpiperaz-in-1-yl) phenyl) prop-2-yn-1-yl)-1-methylpiperidine-4-carboxamide **(11)**.* ^{1}H NMR (300 MHz, DMSO-d_6) δ 9.31 (s, 1H), 8.44 (d, J = 5.6 Hz, 1H), 8.03 (s, 1H), 7.18 (d, J = 2.1 Hz, 2H), 6.82 (d, J = 9.2 Hz, 1H), 5.51 (s, 2H), 4.12 (d, J = 5.4 Hz, 2H), 3.17 (s, 3H), 3.13 (s, 1H), 2.89 (t, J = 4.5 Hz, 4H), 2.52–2.51 (m, 8H), 2.25 (m, 6H), 1.85–1.68 (m, 4H). ^{13}C NMR (75 MHz, DMSO-d_6) δ 173.15, 165.04, 150.73, 147.54, 143.93, 135.54, 135.35, 132.45, 131.97, 128.00, 124.91, 123.32, 120.60, 117.36, 112.71, 112.63, 86.29, 81.41, 54.53, 53.33, 50.77, 45.40, 43.88, 40.35, 28.92, 28.59, 26.68, 11.95, 11.89. HRMS (ESI): calcd. for *m/z* $C_{29}H_{37}ClFN_6O_2$ $[M + H]^+$ 555.2645, found 555.2658. HPLC (80% methanol in water): t_R = 4.077 min, 99.41%. Yield: 61.6%. m.p. 191–194 °C.

*4.1.2.3. 5-amino-2-chloro-4-fluoro-N-(5-(3-(4-hydroxycyclohexanecarboxamido) prop-1-yn-1-yl)-2-(4-methylpiperazin-1-yl) phenyl)-3-methylbenzamide **(12)**.* ^{1}H NMR (300 MHz, DMSO-d_6) δ 9.28 (s, 1H), 8.25 (t, J = 5.3 Hz, 1H), 8.02 (s, 1H), 7.17 (s, 2H), 6.83 (d, J = 9.2 Hz, 1H), 5.48 (s, 2H), 4.53 (d, J = 4.5 Hz, 1H), 4.08 (d, J = 5.4 Hz, 2H), 3.35 (br s, 4H), 2.88 (t, J = 4.6 Hz, 4H), 2.24 (s, 6H), 2.13–1.98 (m, 1H), 1.90–1.78 (m, 2H), 1.72–1.68 (m, 2H), 1.44–1.31 (m, 2H), 1.23 (br s, 1H), 1.16–1.04 (m, 2H). HRMS (ESI): calcd. for *m/z* $C_{29}H_{36}ClFN_5O_3$ $[M + H]^+$ 556.2485, found 556.2492. HPLC (80% methanol in water): t_R = 4.617 min, 95.03%. Yield: 67.4%. m.p. 166–169 °C.

*4.1.2.4. 5-amino-2-chloro-4-fluoro-3-methyl-N-(2-(4-methylpiperazin-1-yl)-5-(3-(2-(te-trahydro-2H-pyran-4-yl) acetamido) prop-1-yn-1-yl) phenyl) benzamide **(13)**.* ^{1}H NMR (300 MHz, DMSO-d_6) δ 9.30 (s, 1H), 8.37 (s, 1H), 8.02 (s, 1H), 7.18 (s, 2H), 6.82 (d, J = 9.2 Hz, 1H), 5.49 (s, 2H), 4.10 (d, J = 5.4 Hz, 2H), 3.81 (d, J = 11.0 Hz, 2H), 3.27 (t, J = 11.5 Hz, 2H), 2.91 (br s, 4H), 2.60 (br s, 4H), 2.32 (s, 3H), 2.25 (d, J = 2.6 Hz, 3H), 2.07–2.05 (m, 2H), 1.56–1.52 (m, 2H), 1.24–1.17 (m, 3H). HRMS (ESI): calcd. for *m/z* $C_{29}H_{36}ClFN_5O_3$ $[M + H]^+$ 556.2485, found 556.2500. HPLC (80% methanol in water): t_R = 5.095 min, 95.34%. Yield: 61.5%. m.p. 117–120 °C.

*4.1.2.5. 5-amino-2-chloro-4-fluoro-N-(5-(3-(5-hydroxypentanamido) prop-1-yn-1-yl)-2-(4-methylpiperazin-1-yl) phenyl)-3-methylbenzamide **(14)**.* Brown oil. ^{1}H NMR (300 MHz, DMSO-d_6) δ 9.27 (s, 1H), 8.30 (t, J = 5.3 Hz, 1H), 8.03 (s, 1H), 7.17 (s, 2H), 6.83 (d, J = 9.3 Hz, 1H), 5.48 (s, 2H), 4.35 (t, J = 5.2 Hz, 1H), 4.10 (d, J = 5.4 Hz, 2H), 3.44–3.33 (m, 2H), 3.32 (br s, 4H), 2.87 (t, J = 4.7 Hz, 4H), 2.28–2.19 (m, 6H), 2.11 (t, J = 7.3 Hz, 2H), 1.60–1.47 (m, 2H), 1.41 (q, J = 6.6 Hz, 2H). HRMS (ESI): calcd. for *m/z* $C_{27}H_{33}ClFN_5NaO_3$ $[M + Na]^+$ 552.2148, found 552.2155. HPLC (80% methanol in water): t_R = 4.485 min, 97.08%. Yield: 64.7%.

*4.1.2.6. 5-amino-N-(5-(3-(2-amino-3-methylbutanamido) prop-1-yn-1-yl)-2-(4-methyl-piperazin-1-yl) phenyl)-2-chloro-4-fluoro-3-methylbenzamide **(15)**.* Brown oil. ^{1}H NMR (300 MHz, DMSO-d_6) δ 9.28 (s, 1H), 8.43 (s, 1H), 8.02 (s, 1H), 7.17 (s, 2H), 6.83 (d, J = 9.2 Hz, 1H), 5.50 (s, 2H), 4.14 (s, 2H), 3.17 (d, J = 3.8 Hz, 2H), 3.06 (d, J = 5.4 Hz, 1H), 2.86 (t, J = 4.7 Hz, 4H), 2.44 (br s, 4H), 2.25 (d, J = 2.6 Hz, 3H), 2.20 (s, 3H), 2.00–1.80 (m, 1H), 0.94–0.79 (m, 6H). HRMS (ESI): calcd. for *m/z* $C_{27}H_{34}ClFN_6NaO_2$ $[M + Na]^+$ 551.2308, found 551.2316. HPLC (80% methanol in water): t_R = 4.052 min, 96.21%. Yield: 60.3%.

*4.1.2.7. N^1-(3-(3-(5-amino-2-chloro-4-fluoro-3-methylbenzamido)-4-(4-methylpiperazi-n-1-yl) phenyl) prop-2-yn-1-yl)-N^4, N^4-dimethylterephthalamide **(16)**.* ^{1}H NMR (300 MHz, DMSO-d_6) δ 9.30 (s, 1H), 9.13 (t, J = 5.4 Hz, 1H), 8.05 (s, 1H), 7.94 (d, J = 8.1 Hz, 2H), 7.49 (d, J = 8.1 Hz, 2H), 7.28–12 (m, 2H), 6.83 (d, J = 9.3 Hz, 1H), 5.48 (s, 2H), 4.35 (d, J = 5.4 Hz, 2H), 2.99 (br s, 4H), 2.90 (s, 6H), 2.55 (d, J = 5.7 Hz, br s, 4H), 2.28 (s, 3H), 2.24 (d, J = 2.6 Hz, 2H). ^{13}C NMR (75 MHz, DMSO-d_6) δ 169.36, 165.33, 165.05, 150.74, 147.54, 143.81, 139.26, 135.53, 135.34, 134.35, 132.43, 131.98, 129.18, 128.05, 127.30, 127.10, 126.81, 125.01, 123.29, 123.07, 120.59, 117.46, 115.56, 112.77, 112.68, 86.34, 81.35, 54.41, 50.58, 45.18, 40.35, 36.40, 34.62, 29.29, 28.94, 11.94, 11.88. HRMS (ESI): calcd. for m/z $C_{32}H_{35}ClFN_6O_3$ [M + H]$^+$ 605.2438, found 605.2450. HPLC (80% methanol in water): t_R = 3.744 min, 99.78%. Yield: 83.4%. m.p. 144–147 °C.

*4.1.2.8. 5-amino-2-chloro-4-fluoro-3-methyl-N-(2-(4-methylpiperazin-1-yl)-5-(3-(4-(morpholine-4-carbonyl) benzamido) prop-1-yn-1-yl) phenyl) benzamide **(17)**.* ^{1}H NMR (300 MHz, DMSO-d_6) δ 9.30 (s, 1H), 9.13 (t, J = 5.5 Hz, 1H), 8.05 (s, 1H), 7.95 (d, J = 8.1 Hz, 2H), 7.51 (d, J = 8.1 Hz, 2H), 7.26–7.12 (m, 2H), 6.82 (d, J = 9.3 Hz, 1H), 5.49 (s, 2H), 4.35 (d, J = 5.4 Hz, 2H), 3.61 (br s, 8H), 2.89 (t, J = 4.7 Hz, 4H), 2.54 (br s, 4H), 2.29–2.20 (m, 6H). HRMS (ESI): calcd. for m/z $C_{34}H_{37}ClFN_6O_4$ [M + H]$^+$ 647.2543, found 647.2548. HPLC (100% methanol): t_R = 3.025 min, 99.46%. Yield: 47.2%. m.p. 120–123 °C.

*4.1.3. Methyl 1-(3-(5-amino-2-chloro-4-fluoro-3-methylbenzamido)-4-(4-methylpipe-razin-1-yl) phenyl)-1H-1,2,3-triazole-4-carboxylate **(18)***

$SnCl_2.2H_2O$ (5.5 g, 24.4 mmol) was added to the solution of compound **44** (2.6 g, 4.9 mmol) in EA (100 mL). The resulting mixture was then refluxed with vigorous stirring for 3 h, and subsequently cooled to room temperature. Following dilution with EA (100 mL) and the mixture was neutralized with saturated sodium bicarbonate solution. Then filtered and washed residue with EA (5 × 40 mL), and the organic phase was separated and dried (Na_2SO_4), filtered, and concentrated. The residue was washed with EA to afford grey white solid **18** (2.3 g). ^{1}H NMR (300 MHz, DMSO-d_6) δ 9.52–9.45 (m, 2H), 8.69 (s, 1H), 7.73 (dd, J = 8.7, 2.7 Hz, 1H), 7.46 (d, J = 8.6 Hz, 1H), 6.92 (d, J = 9.2 Hz, 1H), 5.53 (s, 2H), 3.92 (s, 3H), 3.00–2.90 (m, 4H), 2.51 (br s, 4H), 2.28 (d, J = 2.6 Hz, 3H), 2.24 (s, 3H). HRMS (ESI): calcd. for m/z $C_{23}H_{26}ClFN_7O_3$ [M + H]$^+$ 502.1764, found 502.1774. HPLC (80% methanol in water): t_R = 5.370 min, 96.24%. Yield: 93.9%. m.p. 223–226 °C.

*4.1.3.1. 4-(4-methylpiperazin-1-yl)-3-nitroaniline **(40)**.* To a solution of compound 4-fluoro-3-nitroaniline (6 g, 38.4 mmol) in CH_3CN (50 mL) at room temperature was added *N*-methyl piperazine (5.8 g, 6.3 mL, 57.6 mmol), followed by *N*, *N*-diisopropylethylamine (9.5 mL, 57.6 mmol). After refluxing for 12 h, the reaction mixture was concentrated and purified by column chromatography on silica gel using a common 6% MeOH/DCM gradient to afford compound **40** as red brown solid (8.9 g). ^{1}H NMR (300 MHz, DMSO-d_6) δ 7.06 (d, J = 8.6 Hz, 1H), 6.76 (s, 1H), 6.69 (d, J = 8.5 Hz, 1H), 5.34 (s, 2H), 2.70 (t, J = 4.4 Hz, 4H), 2.27 (br s, 4H), 2.09 (s, 3H). m/z (EI-MS): 259.1 [M + Na]$^+$. Yield: 97.8%. m.p. > 250 °C.

*4.1.3.2. 1-(4-azido-2-nitrophenyl)-4-methylpiperazine **(41)**.* 4-(4-methylpiperazin-1-yl)-3-nitroaniline **40** (4.0 g, 17.0 mmol) was dissolved in an aqueous solution of 2 M HCl (100 mL) in an ice bath. Then $NaNO_2$ (1.76 g, 25.5 mmol in 10 mL of H_2O) was added dropwise. After the reaction mixture was stirred for 30 min at 0 °C, a solution of sodium azide (2.2 g, 34.0 mmol in 10 mL of H_2O) was added dropwise. The reaction mixture was stirred for another 2 h at room temperature. Following by adding 2 M/NaOH to adjust pH = 9–10, red brown solid was precipitated, filtered and dried to give compound **41** (4.0 g). ^{1}H NMR (300 MHz, DMSO-d_6) δ 7.48 (d, J = 2.2 Hz, 1H), 7.34–7.20 (m, 2H), 2.85 (t, J = 4.7 Hz, 4H), 2.31 (t, J = 4.8 Hz, 4H), 2.11 (s, 3H). m/z (EI-MS): 261.1 [M − H]$^-$. Yield: 91.3%. m.p. 88–91 °C.

*4.1.3.3. Methyl 1-(4-(4-methylpiperazin-1-yl)-3-nitrophenyl)-1H-1,2,3-triazole-4-carboxylate **(42)**.* Compound **41** (1.0 g, 3.8 mmol) was added to the solution of methyl propiolate (0.96 g, 11.4 mmol) in MeOH (50 mL) at room temperature. After adding catalyst CuI (0.07 g, 0.38 mmol) and DIPEA (0.12 mL, 0.76 mmol), the mixture was refluxing for 48 h. Filtered to remove unreacted CuI, concentrated, and the residue was washed with EA to afford red brown solid (0.8 g). ^{1}H NMR (300 MHz, DMSO-d_6) δ 9.45 (s, 1H), 8.36 (d, J = 2.7 Hz, 1H), 8.11–8.01 (m, 1H), 7.42 (d, J = 9.1 Hz, 1H), 3.80 (s, 3H), 2.99 (t, J = 5.4 Hz, 4H), 2.35 (t, J = 5.2 Hz, 4H), 2.13 (s, 3H). m/z (EI-MS): 369.2 [M + Na]$^+$. Yield: 61.5%. m.p. 159–161 °C.

*4.1.3.4. Methyl 1-(3-amino-4-(4-methylpiperazin-1-yl) phenyl)-1H-1,2,3-triazole-4-car-boxylate **(43)**.* To a solution of **42** (3.8 g, 12.0 mmol) in MeOH (50 mL), catalytic amount of Palladium/C catalyst was added. The mixture was stirred under H_2 atmosphere at room temperature for 6 h, then the mixture was filtered and concentrated to afford pink solid **43** (3.0 g). ^{1}H NMR (300 MHz, DMSO-d_6) δ 9.28 (s, 1H), 7.28 (d, J = 1.9 Hz, 1H), 7.07 (d, J = 1.9 Hz, 2H), 5.15 (s, 2H), 3.90 (s, 3H), 2.87 (t, J = 4.5 Hz, 4H), 2.53 (br s, 4H), 2.26 (s, 3H). m/z (ESI-MS): 317.1763 [M + H]$^+$. Yield: 78.9%. m.p. 194–197 °C.

*4.1.3.5. Methyl 1-(3-(2-chloro-4-fluoro-3-methyl-5-nitrobenzamido)-4-(4-methylpiper-azin-1-yl) phenyl)-1H-1,2,3-triazole-4-carboxylate **(44)**.* To a solution of **43** (1.7 g, 5.3 mmol) in anhydrous dichloromethane (100 mL) was added 2-chloro-4-fluoro-3-methylbenzoyl chloride **54** (1.6 g, 6.4 mmol) at 0 °C. This was followed by the addition of pyridine (0.43 mL, 5.3 mmol), and the resulting solution was stirred at room temperature for 6 h. The reaction was subsequently filtered and dried to provide light yellow solid **44** (2.6 g). ^{1}H NMR (300 MHz, DMSO-d_6) δ 9.98 (s, 1H), 9.46 (s, 1H), 8.54 (d, J = 2.5 Hz, 1H), 8.36 (d, J = 7.7 Hz, 1H), 7.77 (dd, J = 8.6, 2.7 Hz, 1H), 7.38 (d, J = 8.7 Hz, 1H), 3.90 (s, 3H), 2.98 (t, J = 4.5 Hz, 4H), 2.50 (br s, 4H), 2.43 (d, J = 2.7 Hz, 3H), 2.23 (s, 3H). m/z (EI-MS): 554.2 [M + Na]$^+$. Yield: 92.8%. m.p. 176–179 °C.

*4.1.4. 1-(3-(5-amino-2-chloro-4-fluoro-3-methylbenzamido)-4-(4-methylpiperazin-1-yl) phenyl)-1H-1,2,3-triazole-4-carboxylic acid **(19)***

An aqueous solution of LiOH (1 M, 15 mL) was added dropwise to a solution of compound **18** (2.3 g, 4.6 mmol) in THF (15 mL) at room temperature. THF was removed after the mixture was stirred overnight. The residue was acidified with 2 M HCl and filtered to give white solid (1.7 g). ^{1}H NMR (300 MHz, DMSO-d_6) δ 9.52–9.45 (m, 2H), 8.69 (s, 1H), 7.73 (dd, J = 8.7, 2.7 Hz, 1H), 7.46 (d, J = 8.6 Hz, 1H), 6.92 (d, J = 9.2 Hz, 1H), 5.53 (s, 2H), 3.92 (s, 3H), 3.00–2.90 (m, 4H), 2.50 (br s, 4H), 2.28 (d, J = 2.6 Hz, 3H), 2.24 (s, 3H). HRMS (ESI): calcd. for m/z $C_{22}H_{24}ClFN_7O_3$ [M + H]$^+$ 488.1608, found 488.1617. HPLC (80% methanol in water): t_R = 3.174 min, 98.09%. Yield: 80.4%. m.p. 198–201 °C.

4.1.5. General method for preparation of compounds 20–26

To a solution of **19** (0.18 g, 0.36 mmol) in DMF (10 mL) at room temperature was added BOP reagent (0.32 g, 0.72 mmol), followed by TEA (0.10 mL, 0.72 mmol). The mixture was stirred for 0.5 h before different amines (0.72 mmol) was added. Then the resulting solution was stirred at room temperature for 4–8 h. The aqueous solution was diluted with EA (50 mL) and the mixture was washed

with saturated sodium chloride solution (3 × 30 mL). The organic phase was then separated, dried (Na_2SO_4), filtered, and concentrated to provide crude product. Then purified by column chromatography on silica gel using a common 2–10% MeOH/DCM gradient to afford compounds **20-26.**

*4.1.5.1. 1-(3-(5-amino-2-chloro-4-fluoro-3-methylbenzamido)-4-(4-methylpiperazin-1-yl) phenyl)-N,N-dimethyl-1H-1,2,3-triazole-4-carboxamide **(20)**.* ^{1}H NMR (300 MHz, DMSO-d_6) δ 9.59 (s, 1H), 9.18 (s, 1H), 8.63 (d, J = 2.5 Hz, 1H), 7.71 (dd, J = 8.6, 2.6 Hz, 1H), 7.42 (d, J = 8.6 Hz, 1H), 6.83 (d, J = 9.2 Hz, 1H), 5.50 (s, 2H), 3.11 (br s, 10H), 3.02 (s, 3H), 2.70–2.69 (m, 4H), 2.24 (d, J = 2.5 Hz, 3H). ^{13}C NMR (75 MHz, DMSO-d_6) δ 165.45, 160.61, 150.76, 147.56, 143.96, 143.30, 135.56, 135.37, 133.06, 132.47, 132.42, 132.27, 126.02, 123.31, 123.08, 121.71, 117.04, 115.59, 114.72, 112.78, 112.70, 53.54, 49.40, 43.72, 38.19, 35.50, 28.94, 11.97, 11.91. HRMS (ESI): calcd. for *m/z* $C_{24}H_{29}ClFN_8O_2$ $[M + H]^+$ 515.2080, found 515.2103. HPLC (80% methanol in water): t_R = 5.053 min, 99.06%. Yield: 78.4%. m.p. > 250 °C.

*4.1.5.2. 5-amino-2-chloro-4-fluoro-3-methyl-N-(2-(4-methylpiperazin-1-yl)-5-(4-(morpholine-4-carbonyl)-1H-1,2,3-triazol-1-yl) phenyl) benzamide **(21)**.* ^{1}H NMR (300 MHz, DMSO-d_6) δ 9.61 (s, 1H), 9.24 (s, 1H), 8.64 (d, J = 2.5 Hz, 1H), 7.73 (dd, J = 8.6, 2.6 Hz, 1H), 7.44 (d, J = 8.7 Hz, 1H), 6.86 (d, J = 9.2 Hz, 1H), 5.52 (s, 2H), 4.06 (s, 2H), 3.68 (s, 6H), 3.12 (br s, 8H), 2.69 (s, 3H), 2.26 (d, J = 2.6 Hz, 3H). HRMS (ESI): calcd. for *m/z* $C_{26}H_{31}ClFN_8O_3$ $[M + H]^+$ 557.2186, found 557.2198. HPLC (100% methanol): t_R = 3.193 min, 95.82%. Yield: 67.5%. m.p. > 250 °C.

*4.1.5.3. 1-(3-(5-amino-2-chloro-4-fluoro-3-methylbenzamido)-4-(4-methylpiperazin-1-yl) phenyl)-N-(tetrahydro-2H-pyran-4-yl)-1H-1,2,3-triazole-4-carboxamide **(22)**.* Brown oil. ^{1}H NMR (300 MHz, DMSO-d_6) δ 9.52 (s, 1H), 9.26–9.24 (m, 1H), 8.65 (s, 2H), 7.71 (d, J = 8.7 Hz, 1H), 7.42 (d, J = 9.4 Hz, 1H), 6.89 (s, 1H), 5.53 (s, 2H), 4.06 (s, 1H), 3.9–3.86 (m, 2H), 2.99 (s, 6H), 2.71 (s, 4H), 2.38 (s, 3H), 2.25 (s, 3H), 1.71 (s, 4H). HRMS (ESI): calcd. for *m/z* $C_{27}H_{33}ClFN_8O_3$ $[M + H]^+$ 571.2343, found 571.2358. HPLC (80% methanol in water): t_R = 4.286 min, 99.60%. Yield: 82.9%.

*4.1.5.4. 1-(3-(5-amino-2-chloro-4-fluoro-3-methylbenzamido)-4-(4-methylpiperazin-1-yl) phenyl)-N-(1-methylpiperidin-4-yl)-1H-1,2,3-triazole-4-carboxamide **(23)**.* ^{1}H NMR (300 MHz, DMSO-d_6) δ 9.48 (s, 1H), 9.22 (s, 1H), 8.65 (d, J = 2.6 Hz, 1H), 8.52 (d, J = 8.2 Hz, 1H), 7.70 (dd, J = 8.5, 2.7 Hz, 1H), 7.42 (d, J = 8.6 Hz, 1H), 6.89 (d, J = 9.2 Hz, 1H), 5.54 (s, 2H), 3.78 (s, 1H), 2.92 (t, J = 4.6 Hz, 4H), 2.82–2.78 (m, 2H), 2.26 (d, J = 2.7 Hz, 3H), 2.22 (s, 3H), 2.19 (s, 3H), 2.07–1.86 (m, 4H), 1.75–1.66 (m, 4H). ^{13}C NMR (75 MHz, DMSO-d_6) δ 165.16, 158.86, 150.81, 147.61, 143.97, 143.51, 135.62, 135.44, 133.13, 132.16, 124.67, 123.66, 123.25, 121.69, 116.84, 113.93, 112.89, 54.52, 53.07, 50.91, 45.38, 44.42, 43.81, 40.32, 29.50, 12.00, 11.94. HRMS (ESI): calcd. for *m/z* $C_{28}H_{36}ClFN_9O_2$ $[M + H]^+$ 584.2659, found 584.2665. HPLC (100% methanol): t_R = 3.221 min, 98.28%. Yield: 49.9%. m.p. 240–243 °C.

*4.1.5.5. 1-(3-(5-amino-2-chloro-4-fluoro-3-methylbenzamido)-4-(4-methylpiperazin-1-yl) phenyl)-N-(3-morpholinopropyl)-1H-1,2,3-triazole-4-carboxamide **(24)**.* ^{1}H NMR (300 MHz, DMSO-d_6) δ 9.51 (s, 1H), 9.22 (s, 1H), 8.85 (t, J = 5.8 Hz, 1H), 8.66 (s, 1H), 7.71 (dd, J = 8.6, 2.7 Hz, 1H), 7.43 (d, J = 8.8 Hz, 1H), 6.89 (d, J = 9.2 Hz, 1H), 5.53 (s, 2H), 3.62 (t, J = 4.6 Hz, 4H), 2.98–2.97 (m, 4H), 2.63 (s, 4H), 2.54 (s, 2H), 2.46–2.36 (m, 6H), 2.33 (s, 3H), 2.26 (d, J = 2.6 Hz, 3H), 1.74–1.70 (m, 2H). ^{13}C NMR (75 MHz, DMSO-d_6) δ 165.18, 159.22, 150.84, 147.64, 143.74, 135.59, 135.40, 133.16, 132.26, 124.41, 123.38, 123.16, 121.71, 116.82, 115.58, 114.02, 112.93, 112.85, 65.90, 56.22, 54.34, 53.16, 50.61, 45.74, 45.01, 40.35, 40.08, 37.41, 36.37, 28.93, 25.43, 11.97, 11.91. HRMS (ESI): calcd. for *m/z* $C_{29}H_{38}ClFN_9O_3$ $[M + H]^+$ 614.2765, found 614.2787. HPLC (80% methanol in water): t_R = 4.383 min, 99.54%. Yield: 94.2%. m.p. 135–138 °C.

*4.1.5.6. 5-amino-2-chloro-4-fluoro-3-methyl-N-(2-(4-methylpiperazin-1-yl)-5-(4-(4-methylpiperazine-1-carbonyl)-1H-1,2,3-triazol-1-yl) phenyl) benzamide **(25)**.* ^{1}H NMR (300 MHz, DMSO-d_6) δ 9.50 (s, 1H), 9.19 (s, 1H), 8.64 (d, J = 2.6 Hz, 1H), 7.70 (dd, J = 8.7, 2.6 Hz, 1H), 7.43 (d, J = 8.7 Hz, 1H), 6.89 (d, J = 9.2 Hz, 1H), 5.54 (s, 2H), 4.02 (s, 2H), 3.68 (s, 2H), 2.95 (t, J = 4.5 Hz, 4H), 2.55 (s, 4H), 2.41 (t, J = 5.1 Hz, 4H), 2.32–2.24 (m, 6H), 2.24 (s, 3H). HRMS (ESI): calcd. for *m/z* $C_{27}H_{34}ClFN_9O_2$ $[M + H]^+$ 570.2502, found 570.2505. HPLC (80% methanol in water): t_R = 4.415 min, 99.46%. Yield: 70.2%. m.p. 117–120 °C.

*4.1.5.7. 1-(3-(5-amino-2-chloro-4-fluoro-3-methylbenzamido)-4-(4-methylpiperazin-1-yl) phenyl)-N-(2-morpholinoethyl)-1H-1,2,3-triazole-4-carboxamide **(26)**.* ^{1}H NMR (300 MHz, DMSO-d_6) δ 9.51 (s, 1H), 9.24 (s, 1H), 8.66 (d, J = 2.4 Hz, 1H), 8.56 (t, J = 5.8 Hz, 1H), 7.71 (dd, J = 8.7, 2.6 Hz, 1H), 7.43 (d, J = 8.7 Hz, 1H), 6.89 (d, J = 9.2 Hz, 1H), 5.54 (s, 2H), 3.58 (t, J = 4.6 Hz, 4H), 3.44 (s, 2H), 2.96 (t, J = 4.8 Hz, 4H), 2.59 (s, 4H), 2.54 (s, 2H), 2.44 (s, 4H), 2.30 (s, 3H), 2.26 (d, J = 2.6 Hz, 3H). ^{13}C NMR (75 MHz, DMSO-d_6) δ 165.15, 159.24, 150.85, 147.65, 143.78, 143.60, 135.60, 135.41, 133.17, 132.24, 124.49, 123.39, 123.17, 121.17, 116.85, 115.58, 114.02, 112.95, 112.87, 66.10, 57.14, 54.41, 53.13, 50.71, 45.11, 36.39, 35.61, 28.94, 11.97, 11.91. HRMS (ESI): calcd. for *m/z* $C_{28}H_{36}ClFN_9O_3$ $[M + H]^+$ 600.2608, found 600.2619. HPLC (80% methanol in water): t_R = 4.441 min, 99.07%. Yield: 72.5%. m.p. 195–197 °C.

*4.1.6. Methyl-3'-(5-amino-2-chloro-4-fluoro-3-methylbenzamido)-4'-(4-methylpiper-azin-1-yl)-[1, 1'-biphenyl]-4-carboxylate **(27)***

To a solution of compounds **49** (0.55 mmol) in EA (50 mL) at room temperature was added $SnCl_2.2H_2O$ (0.5 g, 2.2 mmol). The mixture was refluxed with vigorous stirring for 5 h, and subsequently cooled to room temperature. Following dilution with EA (100 mL) and the mixture was neutralized with saturated sodium bicarbonate solution. Then filtered and washed residue with EA (5 × 40 mL), and the organic phase was dried (Na_2SO_4), filtered, and concentrated to afford compounds **27.** ^{1}H NMR (300 MHz, DMSO-d_6) δ 9.33 (s, 1H), 8.39 (s, 1H), 8.04 (d, J = 8.4 Hz, 2H), 7.76 (d, J = 8.3 Hz, 2H), 7.52 ((dd, J = 8.3, 2.0 Hz, 1H), 7.32 (d, J = 8.4 Hz, 1H), 6.88 (d, J = 9.3 Hz, 1H), 5.50 (s, 2H), 3.87 (s, 3H), 2.89 (t, J = 4.4 Hz, 4H), 2.49 (t, J = 4.4 Hz, 4H), 2.25 (d, J = 2.2 Hz, 3H), 2.19 (s, 3H). HRMS (ESI): calcd. for *m/z* $C_{27}H_{29}ClFN_4O_3$ $[M + H]^+$ 511.1907, found 511.1913. HPLC (90% methanol in water): t_R = 6.036 min, 95.06%. m.p. > 250 °C.

*4.1.6.1. Methyl-4'-fluoro-3'-nitro-[1, 1'-biphenyl]-4-carboxylate **(46)**.* Boronic acid (4.3 g, 24.1 mmol) was added to a solution of 4-bromo-1-fluoro-2-nitrobenzene (4.4 g, 20.1 mmol) in dioxane (150 mL). Then Cs_2CO_3 (13.1 g, 40.2 mmol) in water (15 mL) was added into the mixture, follow by a small amount of $Pd(PPh_3)_2Cl_2$. Removing the gas in the reaction bottle and protected with N_2, then the reaction was heated to reflux for 20 h. The mixture was filtered to remove catalytic agent and Cs_2CO_3, then purified by column chromatography on silica gel using a common 1–5% MeOH/DCM gradient to afford compounds **46.** ^{1}H NMR (300 MHz, $CDCl_3$) δ 8.31–8.13 (m, 3H), 7.88–7.59 (m, 1H), 8.28 (m, 3H), 7.42–7.36 (m, 1H), 3.94 (s, 3H). *m/z* (EI-MS): 276.2 $[M]^+$. Yield: 74.2%. m.p. 145–147 °C.

*4.1.6.2. Methyl-4'-(4-methylpiperazin-1-yl)-3'-nitro-[1, 1'-biphenyl]-4-carboxylate **(47)**.* To a solution of compounds **46** (13.8 mmol) in

DMF (30 mL) at room temperature was added N-methyl piperazine (1.8 g, 2.0 mL, 17.9 mmol), followed by N, N-diisopropylethylamine (3.2 mL, 17.9 mmol). The resulting solution was then heated to 80 °C for 2 h, and subsequently cooled to room temperature. Following dilution with EA (150 mL), the mixture was washed with water (3 × 50 mL), then the organic phase was dried (Na_2SO_4), filtered, and concentrate to give target compounds **47**. ^{1}H NMR (300 MHz, $CDCl_3$) δ 8.11 (dd, J = 6.8, 1.9 Hz, 2H), 8.05 (d, J = 2.3 Hz, 1H), 7.44 (dd, J = 8.6, 2.3 Hz, 1H), 7.68–7.61 (m, 2H), 7.46 (m, 2H), 7.21 (d, J = 8.6 Hz, 1H), 3.95 (s, 3H), 3.16 (t, J = 4.7 Hz, 4H), 2.61 (t, J = 4.7 Hz, 4H), 2.38 (s, 3H). *m/z* (ESI-MS): 356.1584 $[M+H]^+$. Yield: 95.5%. m.p. 131–134 °C.

*4.1.6.3. Methyl-3′-amino-4'-(4-methylpiperazin-1-yl)-[1, 1′-biphenyl]-4-carboxylate **(48)**.* To a solution of **47** (12.9 mmol) in EA (50 mL) at room temperature was added $SnCl_2.2H_2O$ (11.6 g, 51.5 mmol). The resulting solution was then refluxed with vigorous stirring for 4 h, and subsequently cooled to room temperature. Following dilution with EA (200 mL) and the mixture was neutralized with saturated sodium bicarbonate solution. Then filtered and washed residue with EA (5 × 40 mL), and the organic phase was dried (Na_2SO_4), filtered, and concentrated to afford compounds **48**. ^{1}H NMR (300 MHz, $CDCl_3$) δ 8.07 (d, J = 8.5 Hz, 2H), 7.61 ((dd, J = 6.7, 1.8 Hz, 2H), 7.09 (d, J = 8.5 Hz, 1H), 7.03 (m, 2H), 4.06 (s, 2H), 3.93 (s, 3H), 3.01 (t, J = 4.4 Hz, 4H), 2.61 (br s, 4H), 2.38 (s, 3H). *m/z* (ESI-MS): 326.1851 $[M+H]^+$. Yield: 98.1%. m.p. > 250 °C.

*4.1.6.4. Methyl-3'-(2-chloro-4-fluoro-3-methyl-5-nitrobenzamido)-4'-(4-methylpipera-zin-1-yl)-[1, 1′-biphenyl]-4-carboxylate **(49)**.* To a solution of **48** (2.4 g, 7.4 mmol) in anhydrous dichloromethane (50 mL) was added 2-chloro-4-fluoro-3-methylbenzoyl chloride **54** (2.2 g, 8.8 mmol) under N_2 atmosphere at room temperature. This was followed by the addition of pyridine (0.71 mL, 8.8 mmol), and the resulting solution was stirred at room temperature for 4 h. The reaction was subsequently diluted with dichloromethane (100 mL) and washed with water (3 × 50 mL) then saturated ammonium chloride solution (2 × 50 mL), then saturated sodium chloride solution (2 × 50 mL). The organic phase was then separated, dried (Na_2SO_4), filtered, and concentrated to provide compounds **49.** ^{1}H NMR (300 MHz, DMSO-d_6) δ 9.85 (s, 1H), 8.37 (d, J = 7.5 Hz, 1H), 8.29 (s, 1H), 8.07–8.01 (m, 2H), 7.80 (d, J = 8.2 Hz, 2H), 7.60 (d, J = 8.4 Hz, 1H), 7.30 (d, J = 8.4 Hz, 2H), 3.88 (s, 3H), 3.17 (s, 3H), 3.00 (br s, 4H), 2.63 (br s, 4H), 2.44 (s, 3H). HRMS (ESI): calcd. for *m/z* $C_{27}H_{27}ClFN_4O_5$ $[M + H]^+$ 541.1649, found 541.1658. HPLC (90% methanol in water): t_R = 6.012 min, 98.45%. Yield: 83.5%. m.p. 193–196 °C.

*4.1.6.5. 3'-(5-amino-2-chloro-4-fluoro-3-methylbenzamido)-4'-(4-methylpiperazin-1-yl)-[1,1′-biphenyl]-4-carboxylic acid **(28)**.* Li(OH) (1 M, 10 mL) was added dropwise to a solution of compound **27** (0.1 g, 0.2 mmol) in THF (15 mL) at room temperature. THF was removed after the mixture was stirred for 2 h. The residue was acidified with 1 M HCl and filtered to give white solid (0.05 g, 0.1 mmol). ^{1}H NMR (300 MHz, DMSO-d_6) δ 9.34 (s, 1H), 8.37 (s, 1H), 8.02 (d, J = 8.1 Hz, 2H), 7.72 (d, J = 8.1 Hz, 2H), 7.50 ((d, J = 6.9 Hz, 1H), 7.31 (d, J = 8.1 Hz, 1H), 6.88 (d, J = 9.5 Hz, 1H), 5.51 (s, 2H), 2.93 (br s, 4H), 2.54 (br s, 4H), 2.25 (br s, 6H). HRMS (ESI): calcd. for *m/z* $C_{26}H_{27}ClFN_4O_3$ $[M + H]^+$ 497.1728, found 497.1739. HPLC (80% methanol in water): t_R = 4.754 min, 98.77%. Yield: 50.3%. m p. 194–197 °C.

4.1.7. General procedure for the synthesis of 29–30

To a solution of **28** (0.15 g, 0.30 mmol) in DMF (10 mL) at room temperature was added BOP reagent (0.20 g, 0.45 mmol), followed by TEA (0.13 mL, 0.90 mmol). The mixture was stirred for 0.5 h before different amines (0.45 mmol) was added. Then the resulting solution was stirred at room temperature for 6–10 h. The aqueous solution was poured into 100 mL water and white precipitated solid was filtered off, washed with water, and dried to afford products **29-30.**

*4.1.7.1. 3'-(5-amino-2-chloro-4-fluoro-3-methylbenzamido)-N, N-dimethyl-4'-(4-methl-piperazin-1-yl)-[1,1′-biphenyl]-4-carboxamide **(29)**.* ^{1}H NMR (300 MHz, DMSO-d_6) δ 9.37 (s, 1H), 8.35 (s, 1H), 7.66 (d, J = 7.7 Hz, 2H), 7.51–7.48 (m, 3H), 7.31 (d, J = 7.7 Hz, 1H), 6.86 (d, J = 9.3 Hz, 1H), 5.50 (s, 2H), 2.98 (br s, 10H), 2.77 (br s, 4H), 2.43 (s, 3H), 2.25 (s, 3H). HRMS (ESI): calcd. for *m/z* $C_{28}H_{32}ClFN_5O_2$ $[M + H]^+$ 524.2223, found 524.2217. HPLC (90% methanol in water): t_R = 4.242 min, 95.20%. Yield: 31.8%. m.p. 148–151 °C.

*4.1.7.2. 5-amino-2-chloro-4-fluoro-3-methyl-N-(4-(4-methylpiperazin-1-yl)-4'-(morph-oline-4-carbonyl)-[1,1′-biphenyl]-3-yl) benzamide **(30)**.* ^{1}H NMR (300 MHz, DMSO-d_6) δ 9.33 (s, 1H), 8.36 (s, 1H), 7.67 (d, J = 7.7 Hz, 2H), 7.52–7.45 (m, 3H), 7.31 (d, J = 7.9 Hz, 1H), 6.87 (d, J = 8.9 Hz, 1H), 5.52 (s, 2H), 3.60 (br s, 8H), 3.35 (br s, 4H), 2.90 (br s, 4H), 2.24 (s, 3H), 2.23 (s, 3H). HRMS (ESI): calcd. for *m/z* $C_{30}H_{34}ClFN_5O_3$ $[M + H]^+$ 566.2329, found 566.2321. HPLC (90% methanol in water): t_R = 4.218 min, 96.75%. Yield: 40.8%. m.p. 146–149 °C.

4.10 The detailed synthesis procedures of compound 31 and 32 were listed in the supporting information or see reference [28].

*4.1.7.3. N-(3'-(5-amino-2-chloro-4-fluoro-3-methylbenzamido)-4'-(4-methylpiperazin-1-yl)-[1,1′-biphenyl]-4-yl)-1-methylpiperidine-4-carboxamide **(31)**.* ^{1}H NMR (300 MHz, DMSO-d_6) δ 10.03 (s, 1H), 9.28 (s, 1H), 8.35 (s, 1H), 7.71 (d, J = 8.2 Hz, 2H), 7.54 (d, J = 8.7 Hz, 2H), 7.40 (d, J = 8.2 Hz, 1H), 7.28 (d, J = 8.6 Hz, 1H), 6.89 (d, J = 8.9 Hz, 1H), 5.50 (s, 2H), 3.00–2.96 (m, 2H), 2.88 (t, J = 4.8 Hz, 4H), 2.50 (br s, 6H), 2.31 (s, 3H), 2.28–2.21 (m, 6H), 2.16–2.12 (m, 1H), 1.80–1.70 (m, 4H). HRMS (ESI): calcd. for $C_{32}H_{39}ClFN_6O_2$ *m/z* $[M + H]^+$ 593.2802, found 593.2812. HPLC (100% methanol): t_R = 3.145 min, 98.63%. Yield: 41.7%. m.p. > 250 °C.

*4.1.7.4. N-(3'-(5-amino-2-chloro-4-fluoro-3-methylbenzamido)-4'-(4-methylpiperazin-1-yl)-[1,1′-biphenyl]-4-yl) tetrahydro-2H-pyran-4-carboxamide **(32)**.* ^{1}H NMR (300 MHz, DMSO-d_6) δ 10.00 (s, 1H), 9.38 (s, 1H), 8.29 (s, 1H), 7.71 (d, J = 8.4 Hz, 2H), 7.56 (d, J = 8.4 Hz, 2H), 7.44 (dd, J = 8.3, 2.2 Hz, 1H), 7.29 (d, J = 8.3 Hz, 1H), 6.86 (d, J = 9.2 Hz, 1H), 5.49 (s, 2H), 3.97–3.85 (m, 2H), 3.40–3.31 (m, 4H), 3.15 (br s, 2H), 3.08 (br s, 4H), 2.71 (s, 3H), 2.66–2.53 (m, 1H), 2.26 (d, J = 2.6 Hz, 3H), 1.77–1.65 (m, 4H). HRMS (ESI): calcd. for *m/z* $C_{31}H_{36}ClFN_5O_3$ $[M + H]^+$ 580.2485, found 580.2495. HPLC (80% methanol in water): t_R = 7.116 min, 95.45%. Yield: 91.9%. m.p. > 250 °C.

4.2. Biology

4.2.1. Fluorescence polarization competition assay

All fluorescence polarization (FP) assays were performed on a SpectraMax multi-mode microplate reader (Molecular Devices) using the excitation and emission filters appropriate for each fluorophore used in the binding experiment. The plates used for FP measurements were black nonbinding surface Corning *3757* 384-well plates with 60 μL of assay solution per well, consisting of 20 μL of 3 nM 10mer-Thr-FAM probe, 20 μL of 8 nM WDR5 protein and 20 μL of buffer or an inhibitor sample of varying concentrations and incubated for 30 min. For fluorescein, 485 nm excitation and 535 nm emission filters were used. The IC_{50} value were analyzed by Graphpad prism 6.0 software.

4.2.2. Isothermal titration calorimetry (ITC)

The Isothermal titration calorimetry (ITC) was carried out at 25 °C with the ITC200 system (MicroCal). The compounds were injected into the sample cell containing 300 μL of 20 μM WDR5 by using 2 μL injection with a total 19 injections at 2.5 min intervals from a stirring syringe (750 rpm) into the sample cell. The data were analyzed with the program Origin, version 7.0, supplied by MicroCal.

4.2.3. In vitro MLL HMT functional assay

The MLL1 enzymatic reactions were conducted at room temperature for 60 min in a 50 μL mixture containing methyltransferase assay buffer (50 mM HEPES, 100 mM NaCl, 1.0 mM EDTA, and 5% glycerol, pH 7.8), 1 μM S-adenosylmethionine (SAM), MLL protein complex and the test compound. These 50 μl reactions were carried out in wells of a Histone substrate pre-coated plate. Blocking Buffer was added to stop the methylation reactions for 10 min. Then, 100 μl of diluted primary antibody was added and slowly shaken for 60 min at room temperature. As before, the plate was emptied and washed three times, and shaken with Blocking Buffer for 10 min at room temperature. After discarding the Blocking Buffer, 100 μl of diluted secondary antibody was added. The plate was then slowly shaken for 30 min at room temperature. As before, the plate was emptied and washed three times, and shaken with Blocking Buffer for 10 min at room temperature. Blocking Buffer was discarded and a mixture of the HRP chemiluminescent substrates was freshly prepared. 100 μl of this mixture was added to each empty well. Immediately, the luminescence of the samples was measured in a BioTek SynergyTM 2 microplate reader. The IC_{50} values were calculated using nonlinear regression with normalized dose-response fit using GraphPad Prism 6.0. IC_{50} values represent three independent replicate determinations ± the standard deviation.

4.2.4. AlphaScreen assay

To verify whether compound **63** has good MLL1 HMT selectivity, the AlphaScreen assay was used to evaluated the compound's activity on other methyltransferases (G9a, Dot1L, EZH2, PRMT5, SET8). The AlphaScreen IgG kit provides the necessary reagents for the test. The test was performed in a 384-well white plate (PerkinElmer). The buffer solution contained 10 mM PBS, compound **63**, SAM and proteins mixed at room temperature for 30 min. 5 μL of receptor beads and 5 μL of the substrate antibodies were then added to the reaction system after the enzymatic reaction and incubated for 30 min at room temperature, and 10 μL of AphaScreen Streptavidin coupled donor beads were added. The 384-well white plate was investigated in an AlphaScreen microplate reader (EnSpire Alpha 2390 Multilabel Reader, PerkinElmer).

4.2.5. Cell-based antiproliferative activity studies

To assess cell anti-proliferative activity and cell viability, MV4-11 leukemia cells carrying MLL-AF4 fusion, MOLM-13 leukemia cells carrying MLL-AF9 fusion, K562 cells carrying no MLL fusion were seeded 8000 cells/well in 96-well plates and treated with compounds for 72h at different concentrations, in culture media containing 0.2% DMSO as the final concentration. The cell viability was assessed by CCK8 (WST-8, 2-(2-methoxy 4-nitro phenyl)-3-(4-nitro phenyl)-5- (2, 4-disulfonic acid benzene) -2H − tetrazolium monosodium salt) and the absorption was measured at 450 nm using Thermo Multiskan Spectrum. To evaluate the safety HUVEC cells was treated with an inhibitor with different concentration for 24h and determined using MTT assay. Cell viability inhibition rates of the inhibitors at each concentration point were calculated using the equation as follows: inhibition rate (%) = [1- (OD_{test} − OD_{blank})/($OD_{conrtol}$ − OD_{blank})] × 100%. The IC_{50} values were calculated using Graphpad Prism 6.0 software.

4.2.6. Western blot analysis

Biomarker modulation was determined by Western blot. MV4-11 cells pretreated with various concentrations of compound **24** or DMSO for 7 days. Cells were collected and lysed in lysis buffer [50 mM Tris-Cl, pH 7.6, 150 mM NaCl, 1 mM EDTA, 1% (m/v) Nonidet P-40 (NP-40), 0.2 mM Phenylmethanesulfonyl fluoride (PMSF), 0.1 mM NaF and 1.0 mM dithiothreitol (DTT)] for 30 min. Then cells were centrifuged again at 12 000 rpm for 20 min at 4 °C. The supernatant was collected, and the protein concentration of the whole cell lysates was determined by BCA assay with Varioskan Flash (Thermo, Waltham, MA) at 567 nm. Samples were stored at -80 °C until use.

50 mg tumors were washed by cold PBS and milled with 300 μL of lysis buffer as described previously for 30 min to obtain total cellular extracts. Then the mixture centrifuged at 12 000 rpm for 20 min at 4 °C, and the supernamants were collected. The total protein concentration was also determined by BCA assay. Samples were stored at - 80 °C until use.

The equal amount of total protein extracts was separated by SDS-PAGE and were electroblotted onto the PVDF membranes (PerkinElmer, Northwalk, CT, USA). After blocking with 5% defatted milk for 1h, membranes were incubated at 37 °C for 1h and then 4 °C overnight with primary antibody. And then the membranes were incubated with a DyLight 800 labeled secondary antibody at 37 °C for 1 h. The membranes were screened through the Odyssey infrared imaging System (LI-COR, Lincoln, Nebraska, USA). Anti-β-actin which was used as internal reference was purchased from Protein Tech. Anti- H3K4me1, anti-H3K4me2 and H3K4me3 rabbit polyclonal were obtained from Abcam.

4.2.7. RNA extraction and gene expression analysis

MV4-11 cells were treated with different concentration of compound **24** or DMSO for 7 days. Cells were harvested by centrifugation at 4000 rpm. Total RNA of cells or tumors were isolated using TRIzol (Invitrogen). The concentration of RNA samples was assessed by SpectraMax i3x (Molecular Devices). The RNA was reversely transcribed by using PrimeScript RT reagent kit following the manufacturer's instructions. Real-time PCR ananlysis of *Hoxa9* (HS 151112803_m1), *Meis-1*(HS160306800_m1) was performed using a STEPONE SYSTEM Fast Real Time PCR system. GAPDH was used for normalization. Primers used for RT-PCR are shown as follows: Hoxa9, Sense primer: TACGTGGACTCGTTCCTGCT, antisense primer: CGTCGCCTTGGACTGGAAG; Meis1, Sense primer: GGGCATGGATGGAGT-AGGC, Antisense primer: GGGTACTGATGCGAGTGCAG.

4.2.8. Initial short-time toxicity

Animal experiments were conducted according to protocols approved by Institutional Animal Care and Use Committee of China Pharmaceutical University. The initial short-time toxicity was evaluated in balb/c female mice. The mice were randomized into different groups and intraperitoneally treated with compounds for 10 days. The dose was 80 mg/kg/day. The body weight and death rate were monitored to evaluate the toxicity.

4.2.9. In vivo xenograft study

Animal experiments were conducted according to protocols approved by Institutional Animal Care and Use Committee of China Pharmaceutical University. The *in vivo* antitumor activity was evaluated in female nude mice. MV4-11 (5×10^6) were injected subcutaneously in the right flank. When the average tumor volume reached approximately 100 mm^3, the mice were randomized into different cohorts and intraperitoneally treated every other day for

21 days. Tumor growth and body weight were monitored every 2 days. The tumor volume (TV) was calculated using the formula (smaller diameter)^2 × (larger diameter)/2. The drug efficacy was assessed by calculating the GI% = [1-(TVt-TV_0)/(CVt-CT_0)] × 100%, where TV_t and CV_t are the tumor volume of treatments group and control group measured at each time point, TV_0 and CV_0 are the tumor volume of treatments group and control group monitored at the beginning. The drug efficacy was also assessed by calculating TGI% = (mean $W_{control}$ − mean W_{tumor})/mean $W_{control}$ × 100%. The pharmacodynamic biomarkers were evaluated by Western Blot and RT-PCR as described before.

4.2.10. Subacute toxicity evaluation in normal mice

Female ICR mice (6–8 weeks) were divided into 4 groups (n = 6) in random: control group, **24** efficacious dose group (80 mg/kg), **24** middle-dose group (200 mg/kg), **24** high-dose group (300 mg/kg). All mice were administered *ip* with the corresponding dose every day for 14 days. The body weights of all mice were measured and recorded. All of the mice were dissected at D15, and the heart, liver, spleen, lung, and kidney were extract. The weights of the organs were measured, and the organs were examined by hematoxylin-eosin staining.

4.3. Docking

Docking study was carried out using GOLD5.1. The 3D conformation was generated by the "Prepare Ligand" protocol at pH 7.0. and prepared by Discovery Studio 4.0 (DS 4.0) with CHARMm. The protein structure of WDR5 was downloaded from PDB (4IA9) and was edited by adding hydrogen, deleting unnecessary waters and ligands. Water 536, 557, 677 and 703 were retained in protein, which play vital roles in **WDR5-47** binding to WDR5 [25]. The binding sites were defined according the endogenous ligand **WDR5-47**. The high fitness score model was selected to analyze binding model.

4.4. Physicochemical properties

The solubility of representative compounds was determined on Gemini Profiler instrument (pION) by the "gold standard" Avdeef-Bucher potentionmetric titration method. Permeability (Pe) was determined by a standard parallel artificial membrane permeability assay (PAMPA by pION). PAMPA was conducted on a PAMPA Explorer instrument (pION Inc., Woburn, MA) with PAMPA Explorer command software (Version 3.7.4.1) as follows: test compounds stock was diluted with system solution buffer, pH 7.4 (pION Inc., Woburn, MA) to make diluted test compounds at 10 mM concentration. Subsequently, 150 μL of diluted test compound was transferred to a UV plate (pION Inc., Woburn, MA), and the UV spectrum was read as the reference plate. The membrane on a preloaded PAMPA sandwich (pION Inc., Woburn, MA) was painted with 5 μL of GIT lipid (pION Inc., Woburn, MA). The acceptor chamber was then filled with 200 μL of acceptor solution buffer (pION Inc., Woburn, MA), and the donor chamber was filled with 200 μL of diluted test compound. Then the PAMPA sandwich was assembled at 25 °C for 4 h. The UV spectrum (240–500 nm) of the donor and the acceptor were read. The permeability coefficient was calculated using PAMPA Explorer command software (Version 3.7.4.1) based on the AUC of the reference plate, the donor plate, and the acceptor plate. All compounds were tested in quadruplicate, and the data were presented as mean value. Standards for this assay using propranolol (110.8×10^{-6} cm/s).

Author contributions

The manuscript was written through contributions of all authors. All authors have given approval to the final version of the manuscript.

Declaration of competing interest

The authors declare that they have no known competing financial interests or personal relationships that could have appeared to influence the work reported in this paper.

Acknowledgements

This work was supported by the project 81872799, 81930100 and 81773639 of National Natural Science Foundation of China, the Natural Science Foundation of Jiangsu Province of China (No. BK 20191321), Project Program of State Key Laboratory of Natural Medicines, China Pharmaceutical University (No. SKLNMZZ202003), CPU2018GY02 of Double First Class Innovation Team of China Pharmaceutical University, Project Funded by the Priority Academic Program Development of Jiangsu Higher Education Institutions, the Natural Science Research Project of Jiangsu Higher Education (20KJB350001) and Science and Technology Development Fund of Nanjing Medical University (NMUB2019016).

Appendix A. Supplementary data

Supplementary data to this article can be found online at https://doi.org/10.1016/j.ejmech.2021.113677.

References

[1] Y.L. Dou, T.A. Milne, A.J. Tackett, E.R. Smith, Fukuda, J. Wysocka, C.D. Allis, B.T. Chait, J.L. Hess, R.G. Roeder, Physical association and coordinate function of the H3K4 methyltransferase MLL1 and the H4K16 acetyltransferase MOF, Cell 121 (2005) 873–885.
[2] V. Avdic, P. Zhang, S. Lanouette, A. Groulx, V. Tremblay, J. Brunzelle, J.F. Couture, Structural and biochemical insights into MLL1 core complex assembly, Structure 19 (2011) 101–108.
[3] Y.L. Dou, T.A. Milne, A.J. Ruthenburg, S. Lee, J.W. Lee, G.L. Verdine, C.D. Allis, R.G. Roeder, Regulation of MLL1 H3K4 methyltransferase activity by its core components, Nat. Struct. Mol. Biol. 13 (2006) 713–719.
[4] B.D. Crawford, J.L. Hess, MLL core components give the green light to histone methylation, ACS Chem. Biol. 1 (2006) 495–498.
[5] B. Argiropoulos, R.K. Humphries, Hox genes in hematopoiesis and leukemogenesis, Oncogene 26 (2007) 6766–6776.
[6] A.C. Winters, K.M. Bernt, MLL-rearranged leukemias—an update on science and clinical approaches, Front. Pediatr 5 (2017).
[7] A.T. Thiel, P. Blessington, T. Zou, D. Feather, X. Wu, J. Yan, H. Zhang, Z. Liu, P. Ernst, G.A. Koretzky, X. Hua, MLL-AF9-induced leukemogenesis requires coexpression of the wild-type Mll allele, Canc. Cell 17 (2010) 148–159.
[8] T.A. Milne, M.E. Martin, H.W. Brock, R.K. Slany, J.L. Hess, Leukemogenic MLL fusion proteins bind across a broad region of the Hox a9 locus, promoting transcription and multiple histone modifications, Canc. Res. 65 (2005) 11367–11374.
[9] B.P. Mishra, K.I. Ansari, S.S. Mandal, Dynamic association of MLL1, H3K4 trimethylation with chromatin and Hox gene expression during the cell cycle, FEBS J. 276 (2009) 1629–1640.
[10] E. Artinger, B. Mishra, B. Li, K. Zaffuto, C. Cheng, T. Org, H. Mikkola, M. Djabali, P. Ernst, MLL1-dependent pathways and mechanisms that maintain hematopoiesis, Exp. Hematol. 41 (2013) S20.
[11] T.A. Milne, Y. Dou, M.E. Martin, H.W. Brock, R.G. Roeder, J.L. Hess, MLL associates specifically with a subset of transcriptionally active target genes, Proc. Natl. Acad. Sci. U.S.A. 102 (2005) 14765–14770.
[12] Y. Dou, T.A. Milne, A.J. Ruthenburg, S. Lee, J.W. Lee, G.L. Verdine, C.D. Allis, R.G. Roeder, Regulation of MLL1 H3K4 methyltransferase activity by its core components, Nat. Struct. Mol. Biol. 13 (2006) 713–719.
[13] M.S. Cosgrove, A. Patel, Mixed lineage leukemia: a structure–function perspective of the MLL1 protein, FEBS J. 277 (2010) 1832–1842.
[14] P. Ernst, C.R. Vakoc, WRAD: enabler of the SET1-family of H3K4 methyltransferases, Brief. Funct. Genomics. 11 (2012) 217–226.
[15] F. Cao, Y. Chen, T. Cierpicki, Y.F. Liu, V. Basrur, M. Lei, Y.L. Dou, An Ash2L/RbBP5 heterodimer stimulates the MLL1 methyltransferase activity through coordinated substrate interactions with the MLL1 SET domain, PloS One 5 (2010), e14102.
[16] Z. Yang, J. Augustin, C. Chang, J. Hu, K. Shah, C.W. Chang, T. Townes, H. Jiang, The DPY30 subunit in SET1/MLL complexes regulates the proliferation and

differentiation of hematopoietic progenitor cells, Blood 124 (2014) 2025–2033.
[17] J. Wysocka, T. Swigut, T.A. Milne, Y. Dou, X. Zhang, A.L. Burlingame, R.G. Roeder, A.H. Brivanlou, C.D. Allis, WDR5 associates with histone H3 methylated at K4 and is essential for H3 K4 methylation and vertebrate development, Cell 121 (2005) 859–872.
[18] Z. Odho, S.M. Southall, J.R. Wilson, Characterization of a novel WDR5-binding site that recruits RbBP5 through a conserved motif to enhance methylation of histone H3 lysine 4 by mixed lineage leukemia protein-1, J. Biol. Chem. 285 (2010) 32967–32976.
[19] V. Dharmarajan, J.H. Lee, A. Patel, D.G. Skalnik, M.S. Cosgrove, Structural basis for WDR5 interaction (Win) motif recognition in human SET1 family histone methyltransferases, J. Biol. Chem. 287 (2012) 27275–27289.
[20] H. Karatas, E.C. Townsend, D. Bernard, Y. Dou, S. Wang, Analysis of the binding of mixed lineage leukemia 1 (MLL1) and histone 3 peptides to WD repeat domain 5 (WDR5) for the design of inhibitors of the MLL1-WDR5 interaction, J. Med. Chem. 53 (2010) 5179–5185.
[21] H. Karatas, E.C. Townsend, F. Cao, Y. Chen, D. Bernard, L. Liu, M. Lei, Y. Dou, S. Wang, High-affinity, small-molecule peptidomimetic inhibitors of MLL1/WDR5 protein-protein interaction, J. Am. Chem. Soc. 135 (2012) 669–682.
[22] F. Cao, E.C. Townsend, H. Karatas, J. Xu, L. Li, S. Lee, L. Liu, Y. Chen, P. Ouillette, J. Zhu, J.L. Hess, P. Atadja, M. Lei, Z.S. Qin, S. Malek, S. Wang, Y. Dou, Targeting MLL1 H3K4 methyltransferase activity in mixed-lineage leukemia, Mol. Cell. 53 (2014) 247–261.
[23] H. Karatas, Y. Li, L. Liu, J. Ji, S. Lee, Y. Chen, J. Yang, L. Huang, D. Bernard, J. Xu, E.C. Townsend, F. Cao, X. Ran, X. Li, B. Wen, D. Sun, J.A. Stuckey, M. Lei, Y. Dou, S. Wang, Discovery of a highly potent, cell-permeable macrocyclic peptidomimetic (MM-589) targeting the WD repeat domain 5 protein (WDR5)-Mixed lineage leukemia (MLL) protein-protein interaction, J. Med. Chem. 60 (2017) 4818–4839.
[24] G. Senisterra, H. Wu, A. Allali-Hassani, G.A. Wasney, D. Barsyte-Lovejoy, L. Dombrovski, A. Dong, K.T. Nguyen, D. Smil, Y. Bolshan, T. Hajian, H. He, A. Seitova, I. Chau, F. Li, G. Poda, J.F. Couture, P.J. Brown, R. Al-Awar, M. Schapira, C.H. Arrowsmith, M. Vedadi, Small-molecule inhibition of MLL activity by disruption of its interaction with WDR5, Biochem. J. 449 (2013) 151–159.
[25] Y. Bolshan, M. Getlik, E. Kuznetsova, G.A. Wasney, T. Hajian, G. Poda, K.T. Nguyen, H. Wu, L. Dombrovski, A. Dong, G. Senisterra, M. Schapira, C.H. Arrowsmith, P.J. Brown, R. Al-awar, M. Vedadi, D. Smil, Synthesis, optimization, and evaluation of novel small molecules as antagonists of WDR5-MLL interaction, ACS Med. Chem. Lett. 4 (2013) 353–357.
[26] M. Getlik, D. Smil, C. Zepeda-Velazquez, Y. Bolshan, G. Poda, H. Wu, A. Dong, E. Kuznetsova, R. Marcellus, G. Senisterra, L. Dombrovski, T. Hajian, T. Kiyota, M. Schapira, C.H. Arrowsmith, P.J. Brown, M. Vedadi, R. Al-Awar, Structure-based optimization of a small molecule antagonist of the interaction between WD repeat-containing protein 5 (WDR5) and mixed-lineage leukemia 1 (MLL1), J. Med. Chem. 59 (2016) 2478–2496.
[27] F. Grebien, M. Vedadi, M. Getlik, R. Giambruno, A. Grover, R. Avellino, A. Skucha, S. Vittori, E. Kuznetsova, D. Smil, D. Barsyte-Lovejoy, F. Li, G. Poda, M. Schapira, H. Wu, A. Dong, G. Senisterra, A. Stukalov, K.V. Huber, A. Schonegger, R. Marcellus, M. Bilban, C. Bock, P.J. Brown, J. Zuber, K.L. Bennett, R. Al-Awar, R. Delwel, C. Nerlov, C.H. Arrowsmith, G. Superti-Furga, Pharmacological targeting of the Wdr5-MLL interaction in C/EBPalpha N-terminal leukemia, Nat. Chem. Biol. 11 (2015) 571–588.
[28] D.D. Li, W.L. Chen, Z.H. Wang, Y.Y. Xie, X.L. Xu, Z.Y. Jiang, X.J. Zhang, Q.D. You, X.K. Guo, High-affinity small molecular blockers of mixed lineage leukemia 1 (MLL1)-WDR5 interaction inhibit MLL1 complex H3K4 methyltransferase activity, Eur. J. Med. Chem. 124 (2016) 480–489.
[29] D.D. Li, W.L. Chen, X.L. Xu, F. Jiang, L. Wang, Y.Y. Xie, X.J. Zhang, X.K. Guo, Q.D. You, H.P. Sun, Structure-based design and synthesis of small molecular inhibitors disturbing the interaction of MLL1-WDR5, Eur. J. Med. Chem. 118 (2016) 1–8.
[30] D.D. Li, Z.H. Wang, W.L. Chen, Y.Y. Xie, Q.D. You, X.K. Guo, Structure-based design of ester compounds to inhibit MLL complex catalytic activity by targeting mixed lineage leukemia 1 (MLL1)-WDR5 interaction, Bioorg. Med. Chem. 24 (2016) 6109–6118.
[31] F. Wang, K.O. Jeon, J.M. Salovich, J.D. Macdonald, J. Alvarado, R.D. Gogliotti, J. Phan, E.T. Olejniczak, Q. Sun, S. Wang, D.V. Camper, J.P. Yuh, J.G. Shaw, J. Sai, O.W. Rossanese, W.P. Tansey, S.R. Stauffer, S.W. Fesik, Discovery of potent 2-aryl-6,7-dihydro-5 H-Pyrrolo[1,2-a]imidazoles as WDR5 WIN-site inhibitors using fragment-based methods and structure-based design, J. Med. Chem. 12 (2018) 5623–5642.
[32] J. Tian, K.B. Teuscher, E.R. Aho, J.R. Alvarado, J.J. Mills, K.M. Meyers, R.D. Gogliotti, C. Han, J.D. Macdonald, J. Sai, J.G. Shaw, J.L. Sensintaffar, B. Zhao, T.A. Rietz, L.R. Thomas, W.G. Payne, W.J. Moore, G.M. Stott, J. Kondo, M. Inoue, R.J. Coffey, W.P. Tansey, S.R. Stauffer, T. Lee, S.W. Fesik, Discovery and structure-based optimization of potent and selective WD repeat domain 5 (WDR5) inhibitors containing a dihydroisoquinolinone bicyclic core, J. Med. Chem. 63 (2020) 656–675.
[33] E.R. Aho, J. Wang, R.D. Gogliotti, G.C. Howard, J. Phan, P. Acharya, J.D. Macdonald, K. Cheng, S.L. Lorey, B. Lu, S. Wenzel, A.M. Foshage, J. Alvarado, F. Wang, J.G. Shaw, B. Zhao, A.M. Weissmiller, L.R. Thomas, C.R. Vakoc, M.D. Hall, S.W. Hiebert, Q. Liu, S.R. Stauffer, S.W. Fesik, W.P. Tansey, Displacement of WDR5 from chromatin by a WIN site inhibitor with picomolar affinity, Cell Rep. 26 (2019) 2916–2928.
[34] W.L. Chen, D.D. Li, X. Chen, Y.Z. Wang, J.J. Xu, Z.Y. Jiang, Q.D. You, X.K. Guo, Proton pump inhibitors selectively suppress MLL rearranged leukemia cells via disrupting MLL1-WDR5 protein-protein interaction, Eur. J. Med. Chem. 188 (2020) 112027.
[35] X.J. Zhang, Y.H. Lei, T.H. Hu, Y. Wu, Z.H. Li, Z.S. Jiang, C.Y. Yang, L. Zhang, Q.D. You, Discovery of clinical candidate (5-(3-(4-chlorophenoxy)prop-1-yn-1-yl)-3-hydroxypicolinoyl)glycine, an orally bioavailable prolyl hydroxylase inhibitor for the treatment of anemia, J. Med. Chem. 63 (2020) 10045–10060.
[36] Y. Wu, Z.S. Jiang, Z.H. Li, J. Gu, Q.D. You, X.J. Zhang, Click chemistry-based discovery of [3-Hydroxy-5-(1 H-1,2,3-triazol-4-yl)picolinoyl]glycines as orally active hypoxia-inducing factor prolyl hydroxylase inhibitors with favorable safety profiles for the treatment of anemia, J. Med. Chem. 61 (2018) 5332–5349.
[37] M. Citartan, S.C. Gopinath, J. Tominaga, T.H. Tang, Label-free methods of reporting biomolecular interactions by optical biosensors, Analyst 138 (2013) 3576–3592.
[38] A. Avdeef, O. Tsinman, Miniaturized rotating disk intrinsic dissolution rate measurement: effects of buffer capacity in comparisons to traditional wood's apparatus, Pharm. Res. (N. Y.) 25 (2008) 2613–2627.
[39] C.A. Lipinski, F. Lombardo, B.W. Dominy, P.J. Feeney, Experimental and computational approaches to estimate solubility and permeability in drug discovery and development settings, Adv. Drug Deliv. Rev. 23 (1997) 3–25.
[40] A. Patel, V.E. Vought, V. Dharmarajan, M.S. Cosgrove, A conserved arginine-containing motif crucial for the assembly and enzymatic activity of the mixed lineage leukemia protein-1 core complex, J. Biol. Chem. 283 (2008) 32162–32175.
[41] R.C. Trievel, A. Shilatifard, WDR5, a complexed protein, Nat. Struct. Mol. Biol. 16 (2009) 678–680.
[42] T.A. Milne, S.D. Briggs, H.W. Brock, M.E. Martin, D. Gibbs, C.D. Allis, J.L. Hess, MLL targets SET domain methyltransferase activity to Hox gene promoters, Mol. Cell. 10 (2002) 1107–1117.
[43] M.G. Guenther, R.G. Jenner, B. Chevalier, T. Nakamura, C.M. Croce, E. Canaani, R.A. Young, Global and Hox-specific roles for the MLL1 methyltransferase, Proc. Natl. Acad. Sci. U.S.A. 102 (2005) 8603–8608.
[44] F.E. Erfurth, R. Popovic, J. Grembecka, T. Cierpicki, C. Theisler, Z.B. Xia, T. Stuart, M.O. Diaz, J.H. Bushweller, N.J. Zeleznik-Le, MLL protects CpG clusters from methylation within the Hoxa9 gene, maintaining transcript expression, Proc. Natl. Acad. Sci. U.S.A. 105 (2008) 7517–7522.
[45] J. Cai, V.L. Damaraju, N. Groulx, D. Mowles, Y. Peng, M.J. Robins, C.E. Cass, P. Gros, Two distinct molecular mechanisms underlying cytarabine resistance in human leukemic cells, Canc. Res. 68 (2008) 2349–2357.